Hinc patriam sustinet
Instituto Superior de Agronomia
Universidade Técnica de Lisboa

# Physical Stability of a Lactose-Trehalose Matrix for Nano-Encapsulation of β-Carotene by Spray-Drying

**Hugo Ricardo Dias Barreto**

Dissertação para obtenção do Grau de Mestre em
**Engenharia Alimentar**

Orientadora: Prof. Maria Luísa D.M. Beirão da Costa
Orientador Externo: Prof. Yrjö H. Roos

**Lisboa, 2008**

*Is olc an chearc nach scríobann di féin.*

- Irish Saying

**ACKNOWLEDGEMENTS**

To Professor Yrjö H. Roos for accepting me as his student, allowing me an opportunity to work abroad and providing me with a fulfilling learning experience, while being always willing to learn from his students.

To Professor Maria Luísa Beirão da Costa and Doctor Margarida Moldão Martins, of the *Instituto Superior de Agronomia* (Higher Institute of Agronomy) of Lisbon, for their guidance through the first stages of the project and invaluable assistance in writing and analysing the results.

To Dr. Mohammed Kamrul Haque, for guiding me through the laboratory work, and for putting all his theoretical and practical experience at my disposal.

To Mr. Dave Waldron, for having all the answers.

To Thérèse Uniacke, Jonathan O'Regan and Sinéad Heffernan for taking the time to assist me in operating the instruments needed for this project.

To Dr. Alan Kelly, Kaushal Kothari and Antonio Sullo for being extremely helpful in critical moments, probably without knowing it, just by being kind and easy going.

To Jim McNamara, Donal Humphreys and Maurice Conway for a remarkable skill on solving every possible problem on the department, including the ones I created myself.

To Wenbin Lu, Liam O'Connell, Nattiga Silalai, Sandrine Macé, and Feli Ronda, even though we all had our own individual projects, there was always a chance to learn from each other. Above all that, thanks for the great lab work atmosphere and the great multicultural experience.

To Brendan, Patrick, Michael and Hester… sometimes friendship at the end of an exhausting day comes from the most unexpected sources.

To Pedro Oliveira for unlimited kindness and friendship, sheltering me in every sense, during my early days in Cork.

To my Mother and Grandmother for supporting and enduring my ambitions, and to my Father for the inspiring pride in my decision to experiment a different country.

To my Daniela, for her unconditional support, keeping me motivated for the project, while providing me with plenty of motives to go back home.

**ABSTRACT**

The purpose of this work was to study the physical properties of a model sugar system of lactose and trehalose, related to its potential as an encapsulation matrix. The encapsulation was accomplished by spray-drying of an oil-in-water emulsion, with an oil phase with high content of β-carotene, representing the encapsulated molecule. This study aimed to relate the water content of the matrix sugars with the variation of the glass transition temperature ($T_g$) and the occurrence of crystallization over time. The influence of these changes on the structure of the rehydrated emulsion and the carotene content of the powder were also to be assessed. Characterization of physical changes was made by describing sorption behaviour, physical structure of the reconstituted emulsion from the encapsulate, determination of the thermal transition by DSC, DMA and DEA, and microscopical observation of the stored spray-dried powder.

It was shown that the matrix remains stable if kept under an $a_w$ of 0.33 or lower. Higher figures may lower the glass transition to below room temperature, causing spontaneous crystallization and collapse of the matrix structure, thus affecting the flowability of the encapsulate and exposing carotene to the environment. Sorption data of the spray-dried powder fitted fairly to the BET and GAB isotherms, indicating a monolayer moisture of 4.64% and 3.21%, respectively. DSC analysis on lactose-trehalose model sugar systems showed a glass transition temperature of 107.9ºC for anhydrous sample, 55.2ºC for 11% RVP storage and 30,2ºC for 33% RVP. These results could not be correlated to the results from DMA and DEA analysis, due to the highly irregular results shown by these methods. It is suggested that these methods are inadequate for hydrated samples with high $T_g$.

The droplet sizes obtained with ultra-high pressure homogenization, and the physical stability of the lactose-trehalose amorphous matrix are satisfactory. However, it is still necessary to study the encapsulation efficiency of this matrix on this kind of core material, with more appropriate quantitative methods. As for DMA and DEA analysis, further development of the method is needed to establish a reliable relation with the DSC results.

**Keywords:** Encapsulation, Glass transition, DSC, DMA, DEA.

**RESUMO**

Este trabalho teve como objectivo o estudo das alterações físicas de uma mistura-modelo de partes iguais de lactose e trealose, na perspectiva da sua aplicação como matriz de encapsulamento para β-caroteno. O sistema de encapsulamento considerado neste projecto é uma dispersão de óleo vegetal em água, em que o óleo contém β-caroteno e a água contém a matriz dissolvida e caseinato de sódio, que actuou como emulsionante. O encapsulado seco foi produzido por secagem da emulsão em *spray-drier*.

As alterações físicas estudadas estão geralmente associadas às transições térmicas, nomeadamente a temperatura de transição vítrea. Acima desta temperatura, a mobilidade molecular torna-se suficiente para que a matriz cristalize, reduzindo irreversivelmente o efeito de barreira da matriz. O objectivo do estudo foi o de relacionar o teor de humidade na matriz amorfa com a variação da temperatura de transição vítrea ($T_g$) e a ocorrência de cristalização ao longo do tempo. A influência dessas alterações na matriz foi depois relacionada com a variação do teor de caroteno à superfície do encapsulado e a variação da estrutura física da emulsão reconstituída por hidratação.

Previamente à secagem da emulsão, esta foi optimizada, no que respeita à concentração de caseinato de sódio e parâmetros de homogeneização. Foi utilizada uma tecnologia de homogeneização emergente, em que se aplicam pressões ultra-altas (acima de 50 MPa), para conseguir uma dimensão média das partículas de uma escala de nanómetros. Quanto à concentração de caseinato, foram testados os rácios óleo:proteína de 20:1, 15:1 e 10:1; de modo a minimizar o diâmetro médio das gotículas, assegurar uma estabilidade física (resistência à recoalescência) satisfatória e minimizar a degradação de caroteno resultante da homogeneização. Quanto à homogeneização, foram utilizadas pressões na gama entre 50 e 150 MPa de pressão primária e 5 a 15 MPa de pressão secundária do processo.

A caracterização das alterações físicas do encapsulado consistiu na descrição da relação entre a actividade da água do meio e a humidade de equilíbrio do material, com vista à adaptação das isotérmicas de sorção BET e GAB. O encapsulado foi sujeito a um período de armazenamento de 40 dias a várias humidades relativas, e foram efectuadas análises periódicas para observar a variação do conteúdo de

caroteno à superfície e a variação da estrutura física da emulsão reconstituída. As transições térmicas do material foram determinadas por DSC, e também por DMA e DEA. Estas duas análises tinham como objectivo a correlação dos resultados com as temperaturas obtidas por DSC, através da equação de Arrhenius. Por fim, o encapsulado foi observado no fim do período de armazenamento, ao microscópio com luz polarizada, para observar a possível ocorrência de cristalização. Em conjunto com os objectivos principais deste trabalho, foi desenvolvido um método espectrofotométrico para a determinação de β-caroteno em soluções de *n*-hexano. Este método foi utilizado em todas as quantificações de caroteno deste trabalho.

Os resultados permitiram concluir que a matriz se mantém estável se for mantida a um $a_w$ de 0.339 ou inferior. Valores mais altos permitem a transição vítrea a temperaturas inferiores à temperatura ambiente, causando cristalização espontânea da matriz, afectando assim as características funcionais do encapsulado. Os dados de sorção da matriz ajustaram razoávelmente às isotérmicas BET e GAB, indicando uma humidade da monocamada de 4.64% e 3.21%, respectivamente. A análise por DSC indicou uma $T_g$ de 107.9ºC para a amostra anidra, 55.2ºC para um armazenamento a uma pressão relativa de vapor de água de 11% e 30.2ºC para o armazenamento a 33%. Não foi possível correlacionar estes resultados com os dados da DMA e DEA, devido à elevada irregularidade dos resultados obtidos.

As emulsões homogeneizadas a pressões ultra-altas revelaram um diâmetro médio de partículas satisfatório, bem como a estabilidade física das emulsões. No entanto, a influência da pressão secundária do processo não é evidente.

Conclui-se que existe uma vantagem efectiva na utilização da homogeneização a pressões ultra-altas, e que a matriz se mantém íntegra para o período de tempo considerado, se armazenada a uma humidade relativa inferior a cerca de 45%. Contudo, é necessária uma avaliação da eficiência de encapsulamento desta matriz neste tipo de produto, utilizando métodos quantitativos e experimentais mais adequados. Conclui-se também é necessário maior conhecimento para utilização de DMA e DEA neste tipo de materiais, para melhor correlacionar com os resultados obtidos por DSC.

**Palavras-chave:** Encapsulamento, Transição vítrea, DSC, DMA, DEA.

**TABLE OF CONTENTS**

**INDEX OF TABLES**

**INDEX OF FIGURES**

## ABBREVIATIONS

| | |
|---|---|
| **$a_w$** | Water activity |
| **BET** | Brunauer-Emmet-Teller |
| **DEA** | Di-Electrical Analysis |
| **DMA** | Dynamic Mechanical Analysis |
| **DSC** | Differential Scanning Calorimetry |
| **DTA** | Differential Thermal Analysis |
| **E'** | Storage modulus |
| **E''** | Loss Modulus |
| **GAB** | Guggenheim-Anderson-de Boer |
| **NaCas** | Sodium caseinate |
| **RVP** | Relative Vapour Pressure |
| **RMS** | Root Mean Square |
| **SMD** | Sauter Mean Diameter |
| **$T_g$** | Glass transition temperature |
| **w/w** | Weight over weight |
| **ε'** | Di-Electric constant |
| **ε''** | Di-Electric loss factor |

## INTRODUCTION

Encapsulation has been recently growing as a way of preserving sensitive food materials, creating a barrier between the molecule and the environment which causes degradation. The study of the physical structure of the barrier is important to establish under which conditions should the encapsulate be stored, in order to prevent unexpected breakdown of the capsules.

The purpose of this work was to study the physical changes of a model sugar system of equal parts of lactose and trehalose, related to its potential as an encapsulation matrix for β-carotene, a lipossoluble carotenoid. Such physical changes are generally related to the glass transition temperature, which is a very important, moisture dependent thermal transition. Above this temperature, molecular mobility is sufficient for the matrix to crystallize, irreversibly reducing the barrier effect.

The encapsulation system considered in this project is a spray-dried, oil-in-water emulsion. This study aimed to relate the water content of the amorphous matrix sugars with the variation of the glass transition temperature ($T_g$) and the occurrence of crystallization over time. The influence of these changes on the structure of the rehydrated emulsion and on the carotene content of the powder's surface was also to be assessed.

Prior to spray-drying, the feed emulsion was modelled, in terms of emulsifier concentration and homogenization conditions, in order to achieve minimum droplet size, maximum emulsion stability and optimal carotene protection in the homogenization process. For that purpose, ultra-high pressure homogenization was used, which is a recent technology in food production. The sodium caseinate concentrations tested were expressed as oil:protein ratios of 20:1, 15:1 and 10:1. These values are based on the optimal concentration of 15:1 reported by Vega *et al.* (2006) for similar systems, based in milk powders.

Characterization of the spray-dried material's physical changes consisted of a description of the sorption behaviour, with the objective of determining equilibrium moisture content of hydrated samples, and to fit the BET and GAB sorption isotherms to the experimental data. The spray-dried powder was analyzed, to monitor changes in the fraction of carotene that was exposed on the surface, and to detect changes in

the structure of the reconstituted emulsion from the encapsulate. Thermal transitions were detected by Differential Scanning Calorimetry (DSC), and further analyses were made by Dynamic Mechanical Analysis (DMA) and Di-Electrical Analysis (DEA), to correlate with the DSC results, using Arrhenius equation. Finally, the stored encapsulate was observed with a microscope, under polarizing light, to detect crystallization of the matrix.

Alongside with the main guideline of the work, a spectrophotometric method for β-carotene determination in *n*-hexane solutions was developed.

# CHAPTER I – LITERATURE REVIEW

## 1.1. Physical State of Food Solids

According to the needs of the food industry today, one of the most important concerns is extending the shelf-life or storage stability of foods. This can be accomplished by minimizing the rate at which chemical or biological degradation occurs, either by avoiding optimal conditions for the phenomena, or by reducing the availability of the reaction's role-players. There has been some thorough study on the importance of water availability ($a_w$) in the shelf-life of foods, for its role as universal reaction medium and its fundamental role in microbiology, which supports some classic food preservation processes such as drying and addition of humectants (salts or sugar). Another approach is to limit the mobility of the reacting species themselves, controlling their physical state.

The physical state of the food solids is dictated by the physical state of each component and its behaviour as a separate phase. It defines the molecular mobility of the material, thus influencing its rheological and electrical properties, as well as diffusion and glass transition phenomena (Roos, 1995). Apart from water, foods are mainly constituted by carbohydrates, proteins and lipids. The lipid fraction is not physically affected by water, so its phase behaviour is not as complex as the other fractions. The carbohydrates and proteins may exist in three different physical states: solubilized, crystalline or amorphous, all of them greatly affected by water content and temperature.

### 1.1.1. Crystallization

A crystal is a material in a solid state, composed by molecules, atoms or ions that are bound together, forming a regular pattern or lattice. Crystals are well organized, regular frameworks of molecules, connected by covalent, metallic, ionic or molecular forces (Walstra, 2003). Crystallization occurs either from a melted or solubilized solid, which can be a sugar, salt or triacylglycerol (Walstra, 2003). If the starting point is a melted solid, crystals are formed by dropping the temperature below the melting temperature, and in the case of a solubilized solid, it is formed due to supersaturation (Roos, 1995).

Crystallization occurs in three steps, which are nucleation, propagation and maturation. This means that each crystal has a starting location, or nucleus, and further develops into a full grown crystal by addition of molecules. Therefore, it's a phenomenon that depends strongly on molecular mobility and time, and can be induced by increasing the temperature or the moisture content (Roos and Karel, 1991). Another important parameter for crystal formation speed is the melt or solution's viscosity, as it directly influences the internal molecular mobility of the fluid. It has been found that the addition of polymers may delay crystallization of sucrose (Iglesias and Chirife, 1978, *cit. in* Roos and Karel, 1991), and the same effect was observed when fructose was added (Roos and Karel, 1991), related to increased viscosity and the correspondent hampering effect on the molecular mobility, which also explains faster crystallization in low molecular weight sugars than in polymers (Roos, 1995). Some sugars may crystallize as hydrates, i.e. including water molecules in their crystalline structure, and may show phase behaviour very different from anhydride crystals (Roos, 1995). Crystallization of amorphous carbohydrates may be related to browning reactions, stickiness and caking of powders (Roos and Karel, 1991). Crystallization can be detected by microscopic observation of the material, under polarizing light (Roos, 1995); it is possible to run a quantitative analysis of the degree of crystallization of a structure, by using Fourier-Transform Raman spectroscopy (Gunning *et al.*, 1999), or by calculating the ratio between the heats of fusion of a sample and a pure crystalline form (Sutter *et al*, 2007).

### 1.1.2. Amorphous Materials

Amorphous materials, or glasses, are apparently solid due to their degree of molecular aggregation, although there are considerable differences in its internal structure. In fact, a glass is a supercooled liquid of very high viscosity, which exists in a metastable state of a mechanical solid, capable of sustaining its own flow (Levine and Slade, 1992). In amorphous materials, the particles are closely packed, creating a structure where particles show little translational and rotational motion, but without regular molecular density, and less stable than the crystalline state. Translational motion of molecules, i.e. diffusion, is dependent on the molecular radius and the glass viscosity, and it is a common phenomenon to nearly all chemical reactions (Levine and Slade, 1992; Walstra, 2003). Glasses can be created by a quick drop in temperature from the melted state, but the most

common case in food products is a quick drying process (Roos and Karel, 1991), which removes the solvent, not providing enough time to allow crystallization. Many of the food solids are presented in the amorphous state, especially low molecular weight materials like sugars (Roos and Karel, 1991. Typical examples of amorphous foods are dried skim milk, also called skim milk powder, where its main component is glassy lactose and dry cereal products like hard biscuits, breakfast cereals and pasta, where starch is presented in an amorphous state (Walstra, 2003). The amorphous state is a metastable, non-equilibrium state. As a result, many of amorphous materials' physical properties depend largely on temperature, moisture content and time (Levine and Slade, 1992; Roos, 1992, 1995; Roos and Karel, 1991).

### 1.1.3. Glass Transition

An amorphous material kept at sufficiently low temperatures is hard and brittle, much like a glass (Sperling, 1986, *cit. in* Roos, 1995). Increasing the temperature up to a certain point, the structure of the material loosens, thus allowing some molecular mobility. This can be described as a transition between the "glassy" state and the "rubbery" state, and occurs at a temperature known as the glass transition temperature ($T_g$). It can also be described as the transition between a solid-like material and a highly-viscous fluid; in the rubbery state, molecules exhibit translational and rotational motion, whereas such motion in inhibited in the glassy state (Levine and Slade, 1992; Angell, 1988, *cit. in* Ubbink and Krüger, 2006). Even though mobility is effectively blocked in the glassy state, some reorganization may occur with water, gases and small organic molecules (Ubbink and Krüger, 2006). Although there are structural changes, glass forming or disintegration is not to be considered as a thermodynamic phase transition, since a glass is not an equilibrium state, and glass transition temperatures aren't precisely constant (Walstra, 2003). Usually, there is a relation between a low molecular weight and a correspondent low glass transition temperature, and this becomes evident in sugars (Levine and Slade, 1992; Roos and Karel, 1991b). Estimated glass transition temperatures for some food solids are presented in Table 1.1.

Table 1.1: Estimated values of onset glass transition temperatures for pure anhydrous carbohydrates, related to their molar masses. Source: Walstra, 2003; Roos, 1995.

| Compound | Molar Mass (Da) | $T_g$ (ºC) |
|---|---|---|
| Hexoses | | |
| Glycerol | 92 | -93 |
| Fructose | 180 | 7 |
| Galactose | 180 | 30 |
| Glucose | 180 | 31 |
| Disaccharides | | |
| Sucrose | 342 | 70 |
| Maltose | 342 | 87 |
| Lactose | 342 | 101 |
| Trehalose | 342 | 100 |
| Polyols | | |
| Maltitol | 344 | 39 |
| Sorbitol | 182 | -9 |
| Xylitol | 152 | -29 |

The most important changes that occur in glass transition are related to the specific volume, apparent viscosity and enthalpy flow. An illustration of these three properties, both related to the glass transition temperature ($T_g$) and the melting temperature ($T_m$) is shown in Figure 1.1. The variation of the specific volume ($1/\rho$) is better understood if we consider cooling down the liquid across the glass transition temperature; if the liquid is cooled down slowly enough, crystallization occurs, and the specific volume decreases abruptly. As the material is further cooled down, the reduction of specific volume continues, but at a much slower rate. However, if the liquid is cooled down very fast, crystallization is avoided, and the specific volume continues to decrease at the same rate as before, until the $T_g$ is reached. At this point, the specific volume decreases at the same rate as the crystalline solid (Walstra, 2003). The glass transition affects the mechanical properties of the material as a consequence of the increase in molecular mobility, i.e. the diffusion coefficient of molecules. By increasing the temperature across the $T_g$, viscosity decreases drastically, showing what may be considered a plasticizing effect of temperature on the food material (Roos, 1995). The enthalpy of the system is shown in Figure 1.1 as a first order derivative. The narrow peak that occurs at $T_m$ corresponds to the melting of the crystalline structure, whereas the small step that is observed at $T_g$. When a second derivative of the curve is plotted, a peak is shown at the glass transition temperature; for that reason, we speak of a second-order transition, which is characteristic of a glass (Walstra, 2003).

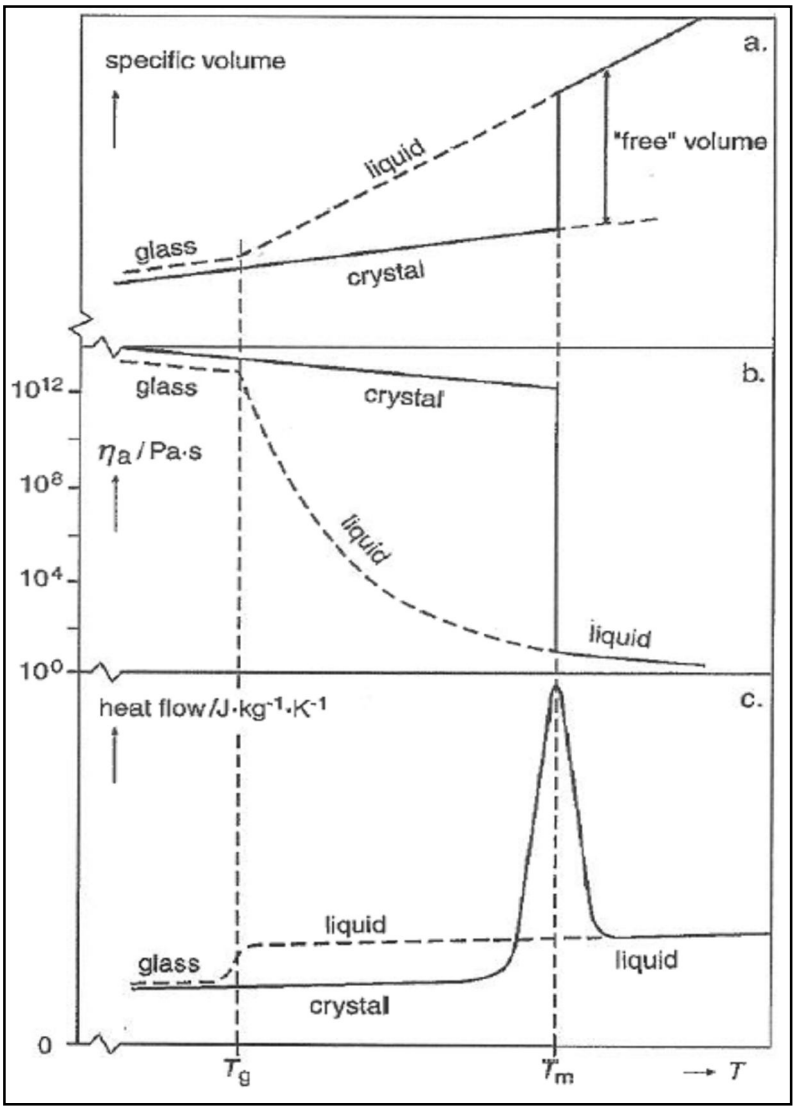


Figure 1.1: Illustration of the glass tran sition, compared to a melting/crystallization of a pure non-polymeric substance. Equilibrium states shown as solid curves and non-equilibrium states are shown as broken curves. (a) Specific volume; (b) Apparent viscosity; (c) enthalpy flow (first derivatives), with the upwards direction representing an endothermic transition. Source: Walstra, 2003.

At temperatures above $T_g$, there is an increase in molecular mobility and a decrease in viscosity, which are sufficient so that crystallization becomes possible, if enough time is allowed (Roos and Karel, 1991); therefore, keeping the environment temperature of amorphous food solids below the $T_g$ is of great importance when controlling storage stability and handling. Frequently, the difficulty relies in controlling the $T_g$ itself, since it's a parameter that is very

sensitive to moisture, and small amounts of water can decrease the material's $T_g$ to a great extent. (Roos and Karel, 1991; Roos, 1995; Vega *et al*, 2006).

### 1.1.4. Water Relations

Water activity ($a_w$) is the most important factor affecting food stability and shelf-life (Roos and Karel, 1991). It is a measure of the availability of water to participate in chemical, microbiological and enzymatic reactions that may cause degradation of foods. Water activity differs from gravimetric water content, because it is related to the vapour pressure exerted by the food's water, and it is a better representative of the influence of water in the food's properties (Walstra, 2003). This vapour pressure depends on the water content, but also on temperature and the composition of food. Some food components, named humectants, are effective in decreasing water vapour pressure in foods; these are usually low molecular weight sugars or salts, but larger molecules may also show activity as humectants, although not as effectively (Lewis, 1996).

When a given food solid is associated with water, the glass transition temperature of the system will decrease (Roos and Karel, 1991), as well as its instant crystallization temperature, although it is more time dependent (Table 1.2). This can be explained by the action of the water as a low molecular weight plasticizer, or its action as a diluent (Roos, 1995). Anyway, it becomes obvious that the material's water content is very important to account for its stability, when it comes to physical changes during processing and storage; as an example, amorphous lactose crystallizes very quickly at room temperature if stored at 40% of relative humidity (Roos and Karel, 1991). Both temperature and moisture content are responsible for plasticization of the amorphous structure, which increases molecular mobility and decreases viscosity, leading to higher reaction rates (Roos and Karel, 1991) However, crystallization rates are reported to depend closer to the temperature disparity towards $T_g$, i.e. the $(T-T_g)$ parameter; at the same $(T-T_g)$ value, the crystallization time is only mildly affected by moisture (Roos, 1992). Empirical examples of glass transition in foods include boiling of pasta, which causes hydration and consequent change into a rubbery material, and loss of crispiness in dry biscuits due to excessive water uptake from the environment (Walstra, 2003).

Table 1.2: Experimental values of onset temperatures for glass transition and crystallization, determined on freeze-dried, amorphous α-lactose and sucrose, hydrated under different water activities. All temperatures are given in ºC. Standard deviation values are omitted. Source: Roos and Karel, 1991.

| Water Activity (25ºC) | Lactose | | Sucrose | |
|---|---|---|---|---|
| | $T_g$ | $T_{cr}$ | $T_g$ | $T_{cr}$ |
| 0,00 | 101,2 | 162,5 | 56,6 | 104,4 |
| 0,11 | 65,0 | 113,3 | 37,4 | 83,7 |
| 0,23 | 43,7 | 93,3 | 27,9 | 75,1 |
| 0,33 | 29,1 | 74,7 | (a) | (a) |
| 0,43 | (a) | (a) | (a) | (a) |

(a) Crystallization occured rapidly at room temperature

Because amorphous carbohydrates are hygroscopic, they will naturally absorb water from the atmosphere, until an equilibrium moisture content is eventually established with the surrounding environment. This phenomenon can be described by sorption isotherms, for any combination of adsorbent (food), adsorbate (water) and temperature (Roos, 1993, *cit. in* Gunning *et al*, 2000). Sorption isotherms, or vapour pressure isotherms, are plots of water content versus $a_w$, and for most foods they exhibit a typical sigmoid-shaped plot (Figure 1.2). The amount of water adsorbed by the food material is related to the specific surface that is exposed, which is related to the higher higroscopicity of fine, amorphous food powders. Knowledge of the sorption isotherms of food materials is very important to have an expression of their higroscopicity, allowing to decide at what air humidity a food material should be stored (Walstra, 2003).

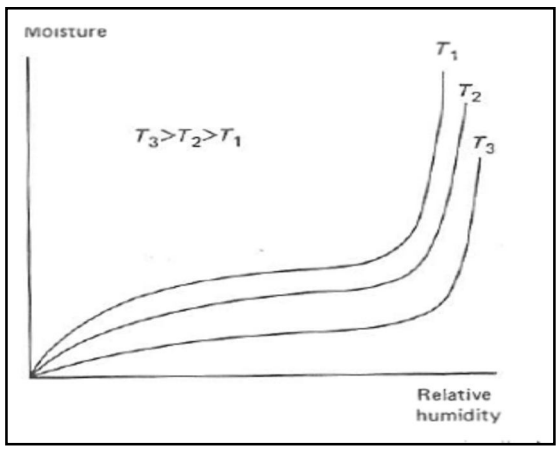


Figure 1.2: Typical sorption isotherms at different temperatures.
Source: Lewis, 1996.

Sorption isotherms are determined by equilibrating samples, usually dehydrated, with air at a known temperature and relative humidity. Controlled relative humidity is commonly accomplished by placing a saturated salt solution in a desiccator, with different relative humidities being provided by different salts, at different temperatures (Table 1.3). The sample is then put inside the desiccator, and its mass is determined at regular intervals, assuming that any increase or decrease is related to water content. Water sorption is affected by temperature, as higher temperatures lead to lower water contents at any environmental relative humidity (Lewis, 1996).

Table 1.3: Water activities of various saturated salt solutions, at 25ºC.
Source: Roos, 1995.

| Salt | Water Activity |
|---|---|
| LiBr | 0,064 |
| LiCl | 0,113 |
| $CH_3COOK$ | 0,225 |
| $MgCl_2$ | 0,328 |
| $K_2CO_3$ | 0,432 |
| $Mg(NO_3)_2$ | 0,529 |
| $NaNO_2$ | 0,654 |
| $SrCl_2$ | 0,709 |
| NaCl | 0,753 |
| $(NH_4)_2SO_4$ | 0,803 |
| KCl | 0,843 |
| $BaCl_2$ | 0,903 |
| $K_2SO_4$ | 0,973 |

In the determination of a sorption isotherm, some deviations may occur. When a food sample is placed under a specific environmental $a_w$, it may take up water from the atmosphere or, if its original moisture is higher, it can release water into the atmosphere. For most foods, the adsorption isotherm doesn't match the desorption isotherm, which means that the relation between relative humidity and equilibrium moisture content is dependent on whether the sample is hydrating or dehydrating. Such phenomenon is known as hysteresis (Lewis, 1996). Another deviation is crystallization of some sugars. Amorphous sugars take up much more water than crystalline sugars, because of their higher higroscopicity. However, if amorphous sugars are allowed to hydrate, and sufficient time is provided, they may crystallize. In sorption isotherms crystallization is shown as an

abrupt decrease in moisture content. During crystallization, water is released, which promotes further crystallization on the remaining non-crystallized fraction. (Roos and Karel, 1991; Roos, 1995). Amorphous samples crystallize before an equilibrium is reached, so they are considered inadequate for sorption studies (Omar and Roos, 2007a).

Examples of mathematical models of isotherms include the Brunauer-Emmett-Teller (BET) isotherm, and the Guggenheim, Anderson-DeBoer (GAB) isotherm. The first isotherm is adequate for monolayer adsorption of water, best fitted under the 0.1-0.5 $a_w$ range, while the GAB isotherm is more versatile to data of various $a_w$ ranges, temperatures and materials, also providing information on monolayer water (Laaksonen and Roos, 2000, Omar and Roos, 2007a, Roos, 1995).

BET Isotherm:

$$\frac{a_w}{m(1-a_w)} = \frac{1}{m_1 K} + \frac{K-1}{m_1 K} a_w \qquad (1.1)$$

This is the linear form of the BET model, intended to fit the experimental data by linear regression. In this equation, $a_w$ is the water activity, $m_1$ the monomolecular layer moisture content on dry basis and $K$ is a constant. According to Karel (1975) (*cit. in* Lewis, 1996), amorphous lactose has a monolayer moisture of 6%.

GAB Isotherm:

$$\frac{a_w}{m} = \alpha (a_w)^2 + \beta a_w + \gamma \qquad (1.2)$$

This is a reduced version of the isotherm, intended for simplified data fitting by second-order polynomial regression. Values of □, □ and □ are used to determine further parameters. In this isotherm, a new parameter, $C$, is introduced (Laaksonen and Roos, 2000).

$$C = \frac{\beta - \frac{1}{m_1}}{-2\gamma} \qquad (1.3)$$

$$K' = \frac{1}{m_1 C\gamma} \quad (1.4)$$

$$m_1 = \sqrt{-\frac{1}{4\alpha\gamma - \beta^2}} \quad (1.5)$$

A measure of the extent of the data fitting to the models can be obtained by the relative percentage root mean square, or %RMS. This parameter is easily calculated and can be used to compare experimental data fitting to different mathematical models.

$$\%RMS = \sqrt{\sum_i^N \frac{\left[(m - m')/m\right]^2}{N}} \cdot 100 \quad (1.6)$$

In this equation, *m* is the experimental moisture content (dry basis), *m'* is the moisture content determined by the isotherm and *N* is the number of samples fitted to the model (Omar and Roos, 2007a).

### 1.1.5. Thermal Transition Determination – DSC, DMA and DEA

It is accepted that there is a direct relation between a food material's thermal transitions (glass transition, crystallization and melting), and its physical properties (Roos, 1995). Furthermore, it is related to the materials' functionality as an encapsulation matrix, and stability of the dried products (Roos, 1987). It should be noted that crystallization is a time-dependant phenomenon, and can occur at temperatures below the experimentally determined instant crystallization temperature ($T_{cr}$), if enough time is provided (Karel and Roos, 1991).

The thermal transitions and correspondent phase changes can be detected by differential thermal analysis (DTA) or differential scanning calorimetry (DSC) (Roos, 1987; Lewis, 1996). The reactions that lead to such phase changes are crystallization, melting and freezing, evaporation and some chemical reactions like denaturation of proteins and starch gelatinization (Lewis, 1996). Both methods are based in heating or cooling of a small quantity of sample and a reference material, but while in DTA the same amount of energy is put into both materials, and temperature difference is recorded, in DSC the temperatures of sample and

reference are the same, and the data collected is the amount of heat required. The results are shown in a thermogram, i.e. a plot of heat flow versus temperature, and when a thermal transition occurs, there is an enthalpy change involved in the reaction that is graphically expressed in the thermogram. DSC analysis is usually done in hermetically sealed pans, to avoid water evaporation, which would greatly affect thermal transition temperatures (Roos, 1995). Amorphous materials in food science are subject to relaxation phenomena due to the physical state itself as well as the glass-forming processes. For some samples it is common to run a heating program followed by a cooling program before the actual analysis, in order to minimize the influence of relaxation, in what may be considered as erasing the thermal history of the material (Lewis, 1996; Roos, 1995).

DSC scans of mixtures, especially when biopolymers are involved, don't show a clear glass transition; for that reason, it can be easier to determine $T_g$ by dynamic mechanical analysis (DMA) (Walstra, 2003). This analysis consists in monitoring changes in mechanical modulus over temperature (Roos, 1995), as shown in Figure 1.3. At the glass transition, the increase of the molecular mobility softens the material, and its ability to store energy decreases (Laaksonen and Roos, 2000). In fact, storage modulus (G') is maximum in the glassy state, and it decreases sharply at the glass transition, while loss modulus (G'') shows a peak at the glass transition temperature, and the peak's onset corresponds to the endset temperature of glass transition, measured by DSC (Roos, 1995). Like DSC, dynamic rheological methods also depend on the rate of temperature increase, but also on the deformation frequency during the measurement, which can be related to the dependence on time (Levine and Slade, 1992; Walstra, 2003).

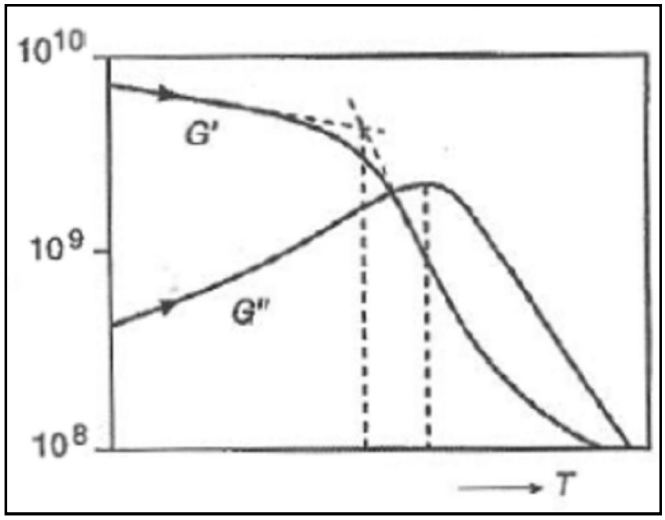


Figure 1.3: Standard scan of storage modulus (G') and loss modulus (G'') versus temperature, for determining the glass transition temperature. Source: Walstra, 2003.

The use of dielectrical thermal analysis (DETA or simply DEA) is, like in DMA governed by changes in storage and loss of energy. In this case, the principle is applied to the ability of the material to store or to conduct an electrical charge, as it is related to molecular mobility (Lievonen and Roos, 2003). The two interesting properties are the relative dielectric constant (ε') and the relative dielectric loss factor (ε''). The variation of these properties, in relation to glass transition, is similar to the mechanical properties determined by DMA (Roos, 1995).

The relative dielectric constant, or relative permittivity, is the ratio of the food material's capacitance and the capacitance of air or vacuum under the same analytical conditions. Capacitance is a measure of the ability of a material to store electrical charge. The SI unit of capacitance is the farad, but since ε' is a relative value, i.e. a ratio of two capacitances, it is dimensionless. The relative dielectrical loss factor is a measure of the amount of energy that is dissipated, i.e. conducted by a material when subjected to an alternating electrical field. It is also a relative value, hence dimensionless. The dielectric constant is related to dipole alignment within the material, while the loss factor is related to the energy required to move dipoles and ions (Lievonen and Roos, 2003). The dielectric properties depend mainly on temperature, physical structure, chemical structure, moisture content and frequency of electric current. Free water and ions have high dielectrical activity, whilst bound water and colloids have low dielectrical activity (Lewis, 1996).

If an alternating, sinusoidal current is applied to a conductor, the resulting current is in the same phase as the applied voltage, and no storage of charge takes place. However, when a capacitor is added, the resulting electrical current is out of phase with the original voltage. The degree of the phase shift is represented as the δ angle, or loss angle, which is 0º for an ideal conductor, and 90º for an ideal capacitor (Figure 1.4). Food materials should show a loss angle between 0º and 90º (Laaksonen and Roos, 2000). The dielectric constant and the dielectric loss factor are related by the loss tangent, or *tan δ*, according to the following equation:

$$\tan\delta = \frac{\varepsilon''}{\varepsilon'} \qquad (1.7)$$

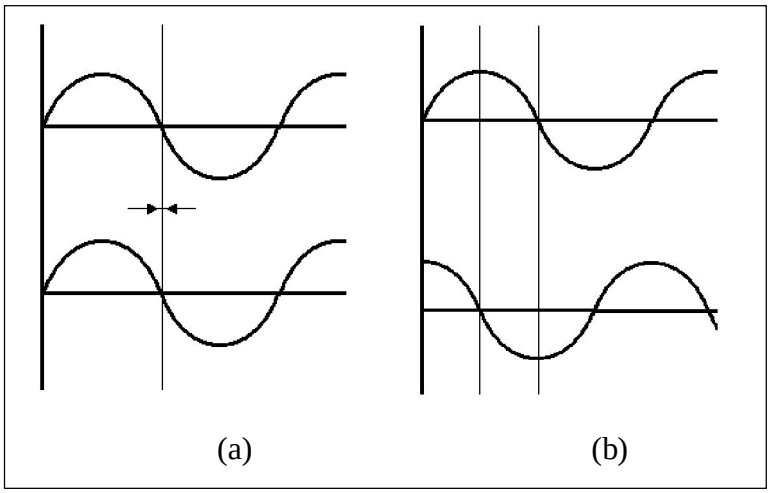


Figure 1.4: Illustration of an ideal conductor (a) and an ideal capacitor (b), related to their phase shift angle. The upper sinusoid represents the applied alternating current, and the lower represents the resulting current.

Both DEA and DMA provide information leading to glass transition temperature. However, the physical changes that indicate the transition are dependent on frequency, whether it is a deformation, in DMA, or an electrical current, in DEA. To find a frequency that correlates to the DSC results, it is necessary to plot experimental temperatures with the correspondent frequency, as Arrhenius functions. This consists in plotting the natural (or Neperian) logarithm of frequency, against the reciprocal absolute temperature, in a linear form of the Arrhenius equation (Talja and Roos, 2001):

$$\ln f = \ln A - \frac{E_a}{RT} \quad (1.8)$$

or

$$\ln f = -\left(\frac{E_a}{R}\right)\frac{1}{T} + \ln A \quad (1.9)$$

In this equation, $f$ is the frequency, $E_a$ is the activation energy, $R$ is the ideal gases constant, $T$ is the absolute temperature and $A$ is a constant.

## 1.2. Encapsulation

### 1.2.1. Overview

Encapsulation is the technique by which a small particle or material is entrapped or enclosed within a continuous material (Soottitantawat *et al*, 2003). The main goal is to establish a physical barrier between the external environment and the entrapped component (Fuchs *et al*, 2005). Encapsulation of active ingredients aims to cope with their sensitivity to a number of physical and chemical factors, like water, oxygen temperature and light, which may cause loss of biological functionality, chemical degradation or inadequate release (Ubbink and Krüger, 2006; Fuchs *et al*, 2005; Pegg and Shahidi, 1999). Such active ingredients include flavourings, colourants, antioxidants, vitamins, preservatives, minerals or, more recently, probiotic microorganisms and various bioactive compounds (Ubbink and Krüger, 2006; Weiss *et al*, 2006).

The continuous materials can either be carbohydrates, gums, polysaccharides, proteins, lipids or biopolymer complexes (Soottitantawat *et al*, 2004; Ubbink and Krüger, 2006), and it must be suitable as an encapsulation matrix. Specifically, it must be easily handled as a vehicle for the sensitive ingredient, must not react with the core material, be compatible with the quality attributes of the other components in the food system and, most importantly, provide an efficient protective effect (Weiss *et al*, 2006; Madene *et al*, 2006). The material's behaviour as an encapsulant depends on its stability, which is on its hand influenced by the chemical nature of the material, ratio of core material to wall material, storage

conditions and encapsulation method (Madene *et al*, 2006). According to the encapsulation process used, the matrix may present several different features that can influence diffusion across the material, both inbound and outbound, with subsequent degradation of the core ingredient. Such features include material shapes (films, spheres, irregular particles), structures (porous or compact) and physical states (crystalline, glassy, rubbery) (Madene *et al*, 2006). Since there is not a single encapsulation matrix that complies with all the characteristics required, it is common to formulate mixtures of carbohydrates, polysaccharides and proteins, in variable proportions (Kaushik and Roos, 2006; Pegg and Shahidi, 1999).

Encapsulation is also a method of controlled delivery of functional ingredients in food systems during processing, storage, or consumption, in this way improving the effectiveness and application range of food additives (Gouin, 2003; Pegg and Shahidi, 1999). In these systems, the encapsulating matrix is designed to collapse under specific environmental conditions, such as pH, ionic strength, temperature or moisture content, thus releasing the encapsulated ingredient. Encapsulates as controlled release systems have long been used by other industries, such as cosmetics and pharmaceutical (Weiss *et al*, 2006). Another well recognized advantage of encapsulation is the conversion of liquid materials, such as essential oils, into easily handled, free flowing powders (Whorton, 1995, *cit. in* Gunning *et al*, 2000; Pegg and Shahidi, 1999; Soottitantawat *et al*, 2003). It can also be seen as a method of extending shelf-life of perishable emulsions, irrespective of the emulsion's physical stability (Vega *et al*, 2006). Furthermore, since encapsulation is frequently a drying process, it may also reduce the volume and weight of the product, thus minimizing the packaging and storage requirements and costs (Vega and Roos, 2005).

The main parameter in dehydrated powder's quality is the composition of the powder surface, since it establishes the bulk behaviour of the powder in terms of wettability, flowability and stability to degradation (Vega, Roos, 2005). These properties may depend on the properties of the wall material, but also on the relative amount of lipids that remain unencapsulated on the powder surface. However, surface lipid content is usually low enough to avoid significant influences on the powder's shelf-life (Fuchs *et al*, 2005; Buffo and Reineccius, 2000, *cit. in* Fuchs *et al*, 2005). Dried powders must also be able to rehydrate into the original

emulsion, with no significant loss of physical structure (Turchiuli *et al*, 2005; Pegg and Shahidi, 1999).

Incorporation of active ingredients in food products is highly complex due to the conditions of most of the food matrices. In other industries, like pharmaceutical, agrochemical or cosmetic, delivery of the active ingredient is the main purpose, and the remaining ingredients can be modelled flexibly. The food industry is subject to a great extent of regulations regarding ingredients, processing methods and storage, and public acceptability must also be considered, in terms of sensory properties, freshness, ease of use, safety and appearance (Ubbink and Krüger, 2006; Weiss *et al*, 2006).

### 1.2.2. Encapsulation Systems and Methods

Encapsulation is generally achieved in a two-stage process. In the first stage, the core material is dispersed within a dense solution of the wall material; the second stage consists of drying or cooling of the emulsion (Madene *et al*, 2006; Minemoto *et al*, 1997). Many sensitive ingredients such as antioxidants, vitamins or flavours are lipid-based or lipossoluble compounds, which exist in liquid form at room temperature. For these lipophilic substances the easiest means of encapsulation consists in a first stage of emulsifying the component in an aqueous solution, often using a homogenizer or high-speed mixer (Soottitantawat *et al*, 2004; Turchiuli *et al*, 2004); the emulsion may be simple oil in water dispersions, or more complex such as multilayered emulsions (Guzey and McClements, 2006).

Encapsulation can be achieved by a number of processes, based on chemical or mechanical principles. The choice of the most suitable method is based on the desired particle size, physical and chemical properties of the matrix, future application of the encapsulate, desired release mechanisms, industrial scale and production costs (Duarte, 2006; Pegg and Shahidi, 1999).

#### 1.2.2.1. Chemical Processes

Coacervation: often regarded as the original method of encapsulation (Risch, 1995, *cit. in* Madene *et al*, 2006), coacervation consists in the formation of an emulsion, followed by physical or chemical precipitation of the continuous

phase around the dispersed phase, which contains the sensitive material, thus forming microcapsules. Residual liquid continuous phase is separated by filtration or centrifugation, the capsules are then washed and, optionally, dried (Vieira, 1998). It's a very promising encapsulation technology due to very high encapsulation efficiency and good controlled release possibilities, based on mechanical stress and temperature (Gouin, 2003).

Co-Crystallization: in this process a supersaturated sugar syrup is held at high temperature, where crystallization becomes spontaneous. If the core material is dispersed in the syrup, small crystals are formed which incorporate the sensitive compounds, either by inclusion, entrapment or simultaneous crystallization (Deladino *et al*, 2006; Madene *et al*, 2006). It has a great advantage of higher wall material stability and low higroscopicity, since the material is in its crystallized state, and also good flowability and dispersion properties (Quellet *et al*, 2001, *cit. in* Madene *et al*, 2006). On the other hand, it has limited use for heat sensitive compounds (Bhandari *et al*, 1998, *cit. in* Madene *et al*, 2006).

Molecular inclusion: in molecular inclusion processes, a sensitive molecule is fitted into and surrounded by the structural network of another molecule (Godshall, 1997, *cit. in* Madene *et al*, 2006). The most documented case of such process is the use of cyclodextrins for encapsulation of flavours (Madene *et al*, 2006; Szente and Szejtli, 2003). Cyclodextrins are the result of cleavage of starch, followed by joining of the edges of the resulting polymer; this is the action of the cyclodextrin glucosyltransferase enzyme (Madene *et al*, 2006). It's a circular molecule with a hydrophobic inner cavity, which is large enough to partially or fully include apolar molecules, such as most of the flavours (Madene *et al*, 2006; Pegg and Shahidi, 1999). The cyclodextrin flavour complexes are highly resistant against oxidation, heat and evaporation (Bhandari *et al*, 1999).

#### 1.2.2.2. Mechanical Processes

Spray-drying: spray-drying is the most widespread method for large-scale encapsulation procedures, due to the relatively low costs, possibility of continuous processing, wide variety of possible matrix materials, and overall

good retention and stability properties of the product (Reineccius, 1989, *cit. in* Madene *et al*, 2006). The principle is to dry an emulsion, solution or suspension, where the sensitive molecule is dispersed in a solution containing the matrix. The emulsion is then spray-dried, i.e. atomized into a chamber where hot air is flowing at high velocity (Figure 1.5), and the small droplets are quickly dehydrated, thus ensuring low particle temperature, despite their contact with hot air (Reineccius, 1994; Gibbs *et al*, 1999). The resulting capsules, collected at the bottom of the drier, are presented as the dispersed phase, coated in an amorphous matrix material (Turchiuli *et al*, 2005; Kaushik and Roos, 2006).

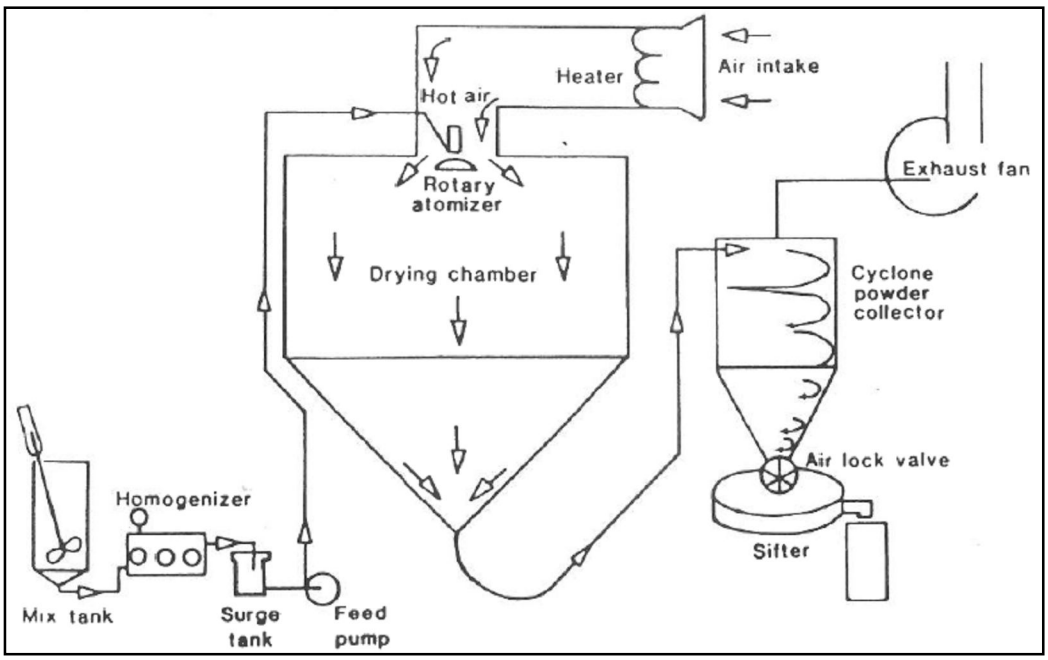


Figure 1.5: A typical spray-drier. Source: Reineccius, 1994.

Although there is heat involved in the process, which may cause loss of volatiles, the temperatures reached are relatively low, which allows this method to be applied to some volatile core materials (Dziezak, 1998, *cit. in* Madene *et al*, 2006). For example spray-drying encapsulation of carotenoid pigments, in gelatine or starch with sucrose, provides a protection effect against degradation (Robert *et al*, 2003, *cit. in* Fuchs *et al*, 2005). The formation of the capsules is based on changes in physical and chemical properties of the matrix and the core material, input flow rate of the drier, drying temperature and the nature of the encapsulating support. Since the emulsion is sprayed through a nozzle, the encapsulating material must be

highly soluble and have low viscosity when in solution, which limits the choice of the wall material (Madene *et al*, 2006; Gouin, 2003). This drying process is liable to leave some of the dispersed droplets uncoated, thus not encapsulating some of the core material, which will remain on the capsules' surface. This not only represents a lowered efficiency of the encapsulation process, but also a potential source of off-flavours due to oxidation (Desobry *et al*, 1997, *cit. in* Madene *et al*, 2006).

The spray-drying method often results in very fine powders, usually in the range of 10-100µm in diameter. Consequently, the material's specific surface is high, which results in quicker hydration of the amorphous matrix. To prevent this, the powder particle size can be increased by agglomeration, using the fluidized bed process (Risch, 1995, *cit. in* Duarte, 2006; Madene *et al*, 2006; Roos, 1995).

Freeze-drying: encapsulation by freeze-drying involves emulsion formation and drying of the continuous phase by sublimation, also known as lyophilization (Minemoto *et al*, 1997). This method is extremely useful when encapsulating thermosensitive substances, since it operates on very low temperatures, unlike the spray-drying method. However, freeze-drying tends to be unattractive, unless for very high value foods, due to the long processing time, and very high costs, up to 50 times higher than that of spray-drying (Desobry *et al*, 1997, *cit. in* Madene *et al*, 2006).

Spray chilling/cooling: spray-cooling and spray-chilling are very similar in principle to spray-drying. The core material is dispersed (emulsified) in a liquefied wall material, and is then atomized through cooling medium, which solidifies the matrix. One essential difference from spray-drying is that no water is withdrawn, which means that the core material must be dispersed in a melt before processing (Risch, 1995, *cit. in* Madene *et al*, 2006).

Since it doesn't involve high temperatures, it is especially suitable for heat sensitive core materials. The typical encapsulating material used with this method is a hydrogenated vegetable oil, with a melting point around 38ºC. However, this method may require special handling and storage conditions in any stage of the process (Madene *et al*, 2006).

Extrusion: encapsulation by extrusion is accomplished by adding the sensitive compound to a low-moisture carbohydrate melt, which is then extruded through small orifices under pressure. The extruded material is then immediately immersed in a cold isopropanol bath, where it attains its glassy state, and is dried in hot air (Reineccius, 1994).

The main advantage of extrusion is its effective protection of oxidation-prone flavours (Madene *et al*, 2006; Gouin, 2006). This method assures that the sensitive material is totally isolated and any remains on the surface are washed away (Gibbs *et al*, 1999). Extrusion is a very convenient method for encapsulation of unstable or volatile components in carbohydrate matrices (Gouin, 2004, *cit. in* Madene *et al*, 2006). However, it is associated with very low retention of volatiles, high production costs and large particle sizes, which can affect food texture (Duarte, 2006). Extruded carbohydrates are also prone to form cracks, thin wall locations or pores that may develop on the material during processing or storage, which may affect barrier properties (Madene *et al*, 2006).

### 1.2.3. Molecular Approach on Encapsulation

Recently, there has been an increasing focus on understanding the molecular mechanisms behind the barrier effect, diffusion, phase transition and structural rearrangement of the matrices (Whorton, 1995, *cit. in* Madene *et al*, 2006). To fully understand the principles of encapsulation, it is crucial to focus on the mechanisms by which volatiles are retained inside a food matrix. In a single-phase system, volatiles are held within the impermeable matrix, which greatly decreases diffusion coefficients, hence their mobility. In a biphasic system, i.e. an emulsion, structure issues are fundamental to volatile release (Gunning *et al*, 1999). Protection of volatiles and controlled release depend mainly on the composition and structure of the wall, which depend not only on the matrix itself, but also on the operating conditions during production and storage of particles (Fuchs *et al*, 2005).

### 1.2.3.1. Release of Encapsulated Molecules

The core materials can have a variety of molecular or physical forms, such as polarities, molecular weights and physical states, which will have a great influence in the location of the encapsulated ingredient. The volatile's affinity for both phases (dispersed and continuous) will determine how it will be partitioned, i.e. a hydrophobic component like a fat of a liposoluble vitamin will form an emulsion in water, while an hydrophilic compound will dissolve in the aqueous phase. This explanation complicates the approach on the release of complex mixtures of core materials, as multiple transport mechanisms must be considered (Gunning *et al*, 1999).

If we consider encapsulation from a biphasic system, where a volatile dissolved in the dispersed phase of an oil-in-water emulsion is encapsulated by the dried continuous phase, the oil droplets will have to be at the surface of the material to release the volatile compound. Considering single-phase systems, the volatile is dissolved within the matrix, and diffusion is the dominant mechanism of release (Gunning *et al*, 1999). Considering these two mechanisms, it is important to note the influence of the partitioning effect of the volatile in a biphasic system; i.e. the solubility of the volatile in the continuous phase, where it behaves locally like in a single-phase system (Gunning *et al*, 1999). If the partitioning effect is irrelevant, and the volatile is fully enclosed behind the matrix, the surface will have to degrade or dissolve for release to occur (Gunning *et al*, 1999; Pothakamury and Barbosa-Canovas, 1995, *cit. in* Madene *et al*, 2006).

### 1.2.3.2. Materials

Carbohydrates are extensively used in spray-dried encapsulation matrices. Such materials include starches, maltodextrins, corn syrup solids and acacia gums, but also proteins and lipids (Madene *et al*, 2006; Pegg and Shahidi, 1999). The advantages of carbohydrates as an encapsulating agent are their diversity, low cost and acceptability, but also the ability to form low viscosity solutions, even at high solids content, which is useful when drying the emulsion (Madene *et al*, 2006). Amorphous carbohydrates in the glassy state

are effective as wall materials, like in milk powders, infant formulas, instant coffee and confectionery products (Ubbink and Krüger, 2006). Encapsulation systems based on glassy carbohydrates have been very effective in minimizing the release of flavours and the oxidation of oxygen-sensitive compounds (Ubbink and Krüger, 2006; Gehl-Hansen and Flink, 1997, *cit. in* Roos and Karel, 1991); this is due to the extremely slow diffusion of molecules, including oxygen, across the glassy matrix. The rates of diffusion depend on the carbohydrate matrix composition, but can also be minimized by lowering water activity, and changing the granule morphology to a larger, less porous structure (Ubbink and Krüger, 2006). Amorphous matrices also provide better rehydration conditions, due to their higroscopicity (Vega and Roos, 2005).

Lactose is a disaccharide, formed by a β-1,4 link between galactose and glucose monomers (Campos, 2002). It is found exclusively in milk, and it is the most widely used matrix for spray-dried systems, as well as the most common pharmaceutical excipient. This is due to its relatively neutral flavour, sufficient solubility and low viscosity of its concentrated solutions (Vega and Roos, 2005). Pure lactose has a glass transition temperature of 107ºC (Miao and Roos, 2004, *cit. in* Vega and Roos, 2005), but small amounts of water are sufficient to decrease this temperature to a great extent, leading to accelerated rates of food degradation (Vega and Roos, 2005). Trehalose is a common name for α,α-trehalose, a non-reducing disaccharide, formed by a 1,1 linkage of two D-glucose molecules. Its technical qualities in cryo-preservation and desiccation protection are regarded as very promising for the food industry, also associated with low production costs (Vega *et al*, 2006). In its anhydrous form it has the same molecular weight as lactose; however, it crystallizes as a dihydrate, which means sufficient water must be available for trehalose to crystallize.

Food proteins are also used as encapsulants, although not as extensively as carbohydrates; such materials include soy protein isolate, whey protein isolate, and sodium caseinate (Kim *et al*, 1996, *cit. in* Madene *et al*, 2006; Baranauskiene *et al*, 2005). These are polymers that show a great variety of chemical groups, hence the ability to associate between themselves and also interact with many other substances, like water, small ions and other

compounds at oil/water interfaces; they also present amphiphilic properties, large molecular weight, and polymer chain flexibility. Food proteins have excellent properties for usage in encapsulation systems, such as high solubility, low viscosity, and good film-forming and emulsifying abilities (Madene *et al*, 2006; Kaushik and Roos, 2006). Sodium caseinate is the result of a disintegrated casein micelle, found in milk. Casein micelles contain 4 different types of protein, $\alpha_{s1}$- $\alpha_{s2}$- β- and κ- caseins, present respectively as 38, 10, 36 and 12% of total casein in bovine milk. They all contain a high level of proline in their primary structure, which prevents the formation of a secondary structure, keeping the molecules linear. Proline also improves the protein's stability to denaturation and surface activity, rendering good emulsifying properties (Vega and Roos, 2005). If found in excess, sodium caseinate can also work as a matrix forming compound in encapsulation systems, apart from its role as an emulsifier.

#### 1.2.3.3. Glass Transition and Crystallization

The study of thermal transitions, especially glass transition, has gained importance as a concept in material science of foods, due to their relation with processing and stability of carbohydrate based foods (Ubbink and Krüger, 2006). Phase transitions like glass transition and crystallization, or other phenomena like caking and melting may be predicted by an adequate selection of the initial formulation of powders (Fuchs *et al*, 2005).

The glass transition temperature is related to volatile release, structural collapse, matrix crystallization and amount of extractable oil (Gunning *et al*, 1999). An amorphous material has the capability to encapsulate as long as it remains in the glassy state; if the temperature is raised above the $T_g$, the material shifts to the rubbery state, causing release of the encapsulated molecules due to structure collapse and crystallization, to the same extent to which storage temperature exceeds glass transition temperature (Roos and Karel, 1991; Gunning *et al*, 1999). Nevertheless, it is possible that changing the material from the glassy to the rubbery state is enough for some of the core material to break through to the surface of the matrix, without the influence of crystallization (Gunning *et al*, 1999). Lipid release from a lactose matrix was also associated with carbohydrate crystallization by Labrousse *et*

*al* (1992, *cit. in* Gunning *et al*, 1999); lipid extractability by solvent was reported to be affected by crystallization of a lactose-based matrix (Moreau and Rosenberg, 1993, *cit. in* Gunning *et al*, 1999). The presence of salts in the amorphous matrix was also reported to lower or raise the glass transition temperature, and to affect the crystallization behaviour of sugars (Omar and Roos, 2007b; Sutter *et al*, 2006).

Amorphous matrices are thermoplastic and hygroscopic, which means that they are sensitive to moisture and temperature changes. As a consequence, they are subject to cohesion and caking, during storage or processing (Vega and Roos, 2005). Caking is a common phenomenon in low molecular weight components, and it is related to flowing of the matrix due to surface tension, in the rubbery state, i.e. it is directly related to the material's glass transition (Slade and Levine, 1995, *cit. in* Gunning *et al*, 2000; Vega and Roos, 2005). However, even assuming that the matrix is kept under appropriate conditions, the free surface oil can be directly responsible for lowered powder handling properties (Vega and Roos, 2005).

Although the main concern when storing is in keeping the materials below the $T_g$, the water and temperature plasticization can be desired to control the release of the encapsulated volatile (Roos and Karel, 1991). It has been reported that the encapsulated volatiles may decrease the crystallization temperature of the amorphous matrix (To and Flink, 1978, *cit. in* Roos and Karel, 1991). It was also reported that collapse temperatures of an encapsulation matrix may be increased by including other materials with higher collapse temperature (Roos, 1987).

#### 1.2.3.4. Physical Properties of Emulsions

An emulsion is a biphasic system of two immiscible liquids, with one of them being distributed as finite globules within the other. Most emulsions are mixtures of oil and water, and both of them can be found as dispersed or continuous phase. An emulsion is considered to be stable if there is no apparent change in the droplet size distribution, droplet aggregation and spatial arrangement (Dickinson, 1994, *cit. in* Vega and Roos, 2005). To improve emulsion stability, i.e. keeping the dispersed phase from recoalescing

and maintaining droplet size, emulsifiers are employed. These work by reducing interfacial tension between both phases, thus reducing the work necessary to produce the emulsion (Lewis, 1996). Emulsifiers can be divided into ionic and non-ionic. Ionic emulsifiers are amphiphilic compounds, i.e. they have both a polar and a non-polar region in their molecular structure, which allows them to link polar with non polar phases. These emulsifiers suffer the disadvantage of reacting with oppositely charged particles, namely metallic ions, which may create complexes of lower solubility and capacity as an emulsifier (Lewis, 1996).

When considering a dispersion or an emulsion, particles or droplets can assume a range of sizes. Concerning encapsulation technology, particle or droplet size of feed emulsions corresponds to the powder particles' size after drying. It has been found that smaller powder and emulsion particle size is related to higher retention of flavours during drying and lower surface oil content (Kaushik and Roos, 2006; Vega and Roos, 2005), although it accounts for lower stability during storage due to increased surface area (Soottitantawat *et al*, 2003, 2004). Particle size reduction can be accomplished by high shear mixing, high-pressure homogenisation, microfludisation and ultrasound emulsification. A distinction is made between high-pressure (up to 50 MPa) and ultra-high pressure (up to 350 MPa) homogenisation; the latter has the advantage of providing enough energy to break droplet clusters apart and disperse them uniformly. Furthermore it is expected that the surface activity of emulsifiers is improved by using ultra-high pressure homogenisation (Kaushik and Roos, 2006).

It is relevant to observe the particle size distribution of emulsions to analyze re-coalescence of droplets over time, i.e. emulsion physical stability. Particle size may be determined in coarse powders by sieving, but in liquid oil-in-water emulsions it is common to used laser diffractometry. Laser diffractometry relates the sizes of particles with the scattering angle of a laser beam that runs across the particle. This gives fairly accurate results, and clear particle size distribution plots. It should be noted that due to the specific nature of this method, results are volume based, i.e. for each particle size, there is a correspondent relative frequency, presented as a percentage of total particle volume. One must also note that all particles are assumed to be equivalent to

spheres; in liquid emulsions, this means no significant error, since particles are originally spherical.

Once the particle size distribution is determined, the following parameters can be defined:

$$S_n = \sum_{i=1} N_i d_i^n \qquad (2.1)$$

$S_n$ is the *n*th moment of the distribution, *d* is the sphere diameter, and *N* is the corresponding number of particles for that diameter.

$$D_{ab} = \left( \frac{S_a}{S_b} \right)^{\frac{1}{(a-b)}} \qquad (2.2)$$

This is a general equation for average diameter. Various values with different meaning can be obtained with different *a* and *b* parameters (Walstra, 2003; Soottitantawat *et al*, 2004).

*Mean diameter,* also called *Number average*:

$$D_{10} = \left( \frac{S_1}{S_0} \right) \qquad (2.3)$$

*Volume average diameter*:

$$D_{30} = \left( \frac{S_3}{S_0} \right)^{\frac{1}{3}} \qquad (2.4)$$

*Volume/surface average diameter*, also called *Sauter Mean Diameter*:

$$D_{32} = \left( \frac{S_3}{S_2} \right) \qquad (2.5)$$

The most commonly used average may be $D_{32}$, or Sauter mean diameter, which is generally very close to the modal volume diameter (Walstra, 2003). Distribution width can be calculated according to equation (2.6) (Christensen *et al*, 2001), where D(v, n) is the volume distribution's percentile of *n*.

$$Span = \frac{D(v,0.9) - D(v,0.1)}{D(v,0.5)} \qquad (2.6)$$

# CHAPTER II – PRELIMINARY EMULSION STUDY AND SELECTION

In the first stage of the study, various formulations and homogenization conditions were tested, in order to achieve a small droplet size and the lowest possible core material destruction in the homogenization process. It is also important that the emulsion remains physically stable, so the particle size distribution was monitored for some days to detect eventual changes in the emulsion structure. In this chapter, the development of the spectrophotometric method for carotene analysis is also included.

## 2.1. Materials and Methods

### 2.1.1. Particle Size Analysis

For this study, lactose and sodium caseinate (NaCas) were supplied by Dairygold (Kerry, Ireland); α,α-trehalose was supplied by Cargill (Minneapolis, USA); the sunflower oil used was of food grade, and was purchased from a local retailer.

The emulsions for this study were prepared according to a basic composition of 10% (w/w) oil and 20% (w/w) total solids (TS). The total solids comprise the emulsifier protein and a mixture of equal proportions of lactose and trehalose. The emulsions were formulated with three different protein contents, all expressed in proportion to the oil content. The purpose was to explore the emulsion properties for the oil:protein ratios around 15:1, which was reported to provide smaller emulsion droplet sizes and structural stability, in model emulsions of anhydrous milk fat with lactose and trehalose (Vega *et al*, 2006). The amount of sugars added to the emulsion was then adjusted, so that its sum with the protein content equalled the desired TS content of 20%. The formulations of the emulsions are summarized in Table 2.1.

Table 2.1: Emulsion formulations used for the preliminary study. All values are given on a weight basis, and based on a 1000 g emulsion.

| Ingredient | Oil:Protein Ratio | | |
|---|---|---|---|
| | 20:1 | 15:1 | 10:1 |
| Lactose | 97,5 | 96,7 | 95,0 |
| Trehalose | 97,5 | 96,7 | 95,0 |
| NaCas | 5,0 | 6,7 | 10,0 |
| Oil | 100 | 100 | 1000 |
| Water | 700 | 700 | 7000 |
| Total Weight | 1000 | 1000 | 1000 |

The mixture of the components was made in different stages. Primarily, bulk sodium caseinate solutions were prepared overnight, at a temperature of 50ºC, maintained with a water bath, with constant stirring at 130 rpm.. Afterwards, the bulk solutions's water content was rectified according to the weight and the solutions were diluted to the appropriate NaCas content. Then the carbohydrates were mixed with intermitent manual stirring, while cooling at room temperature.

The sunflower oil was added immediately prior to mixing of the emulsion to avoid unnecessary water-related degradation of the oil. Mixing was carried out in a Ultraturrax T25 (Janke & Kunkel IKA Labortechnik, Germany) high-shear mixer, set to 13,500 r.p.m. for 1 minute.

All three different compositions were homogenized in a Stansted nm-GEN 7400H High-Pressure Homogenizer (Stansted Fluid Power Ltd., Stansted, UK), using 50, 100 and 150 MPa as pressures for the primary process, and 5, 10 and 15 MPa as secondary homogenization pressures. Primary homogenization consists in dividing the dispersed phase into smaller droplets, whereas the secondary process aims to disperse agglomerated droplets. Samples for all the combinations of composition/primary pressure/secondary pressure were collected, and were analysed for particle size distribution by laser diffractometry with a Malvern Mastersizer S (Malvern Instruments Ltd., Malvern, UK) particle sizer, set to a refractive index of 1.46.

### 2.1.2. Structural Stability Analysis

To study the ability of the sodium caseinate to stabilize the emulsions, the three different emulsion formulations were homogenized under the same conditions. Emulsions of oil-to-protein ratios of 20, 15 and 10 to 1 were processed using primary and secondary pressures of 100 MPa and 10 MPa, respectively. The resulting emulsions were stored at 5ºC and analysed for their particle size distribution over a period of six days, to monitor any eventual change in the emulsion's structure over time, i.e. their droplet distribution profile.

### 2.1.3. Spectrophotometric Method

The spectrophotometric method was established by determination of the calibration curve for β-carotene/n-hexane solutions. β-carotene was purchased from Fluka Biochemie, and n-hexane was supplied by Sigma-Aldrich. The instrument used was a Lambda 35 UV/Visible Spectrometer, by Perkin-Elmer Instruments, USA.

In a first step, a sample of carotene dissolved in hexane was scanned for all the wavelengths between 200 and 600 nm, thus determining the absorbance profile of carotene. The wavelength corresponding to the highest absorbance was selected for the determination of the calibration curve. This second stage consisted in running several samples, with various concentrations of carotene, precisely known. By plotting the absorbance levels according to the carotene concentration, a straight line can be adjusted to a range of concentrations where the plot is linear, and a clear relation between absorbance and concentration is possible (Lambert-Beer Law).

### 2.1.4. Carotene Stability on Homogenization

A single emulsion composition, corresponding to an oil-to-protein ratio of 20:1, was prepared dissolving β-carotene in the sunflower oil, in a proportion of around 0,8mg of carotene per gram of oil. The emulsion was mixed with the same high-shear mixing parameters as before, and then homogenized with the same combinations of primary and secondary process pressures.

The emulsion samples were then extracted with hexane for carotene content determination. Approximately 1g of emulsion was further dispersed with about 8ml of distilled water, and 5.00ml of hexane were added. The mixture was manually shaken in a plastic, screw-cap tube for 30 seconds to allow sufficient contact between hexane and carotene. Afterwards, the samples were centrifuged at a speed of 2000 rpm for 15 minutes in a Gallenkamp CF600 (Gallenkamp, Netherlands) centrifuge. The supernatant hexane phase was analysed by spectrophotometry.

## 2.2. Results

### 2.2.1. Particle Size Analysis

To determine the average droplet diameter, the Sauter Mean Diameter (SMD), or D(3,2), was considered to be the most approximate parameter, since it is generally coincident with the mode in unimodal distributions, i.e. the peak value. It also shows little variation to residual amounts of droplets that show sizes too different from the bulk. Some other parameters, like D(4,3), are greatly affected by small amounts of droplets that represent statistical outliers. A small average droplet size is a key parameter, but a small breadth of droplet sizes is also relevant, as it ensures that the particles show diameters as close as possible to the average value, which also indicates an efective homogenization. Distribution width is presented as the *span* value. Both the distribution span and the Sauter Mean Diameter are given directly by the instrument's software (Mastersizer S 2.15; 1994, Malvern Instruments). All emulsion were analyzed for both parameters, and results are shown in Figures 2.1 and 2.2.

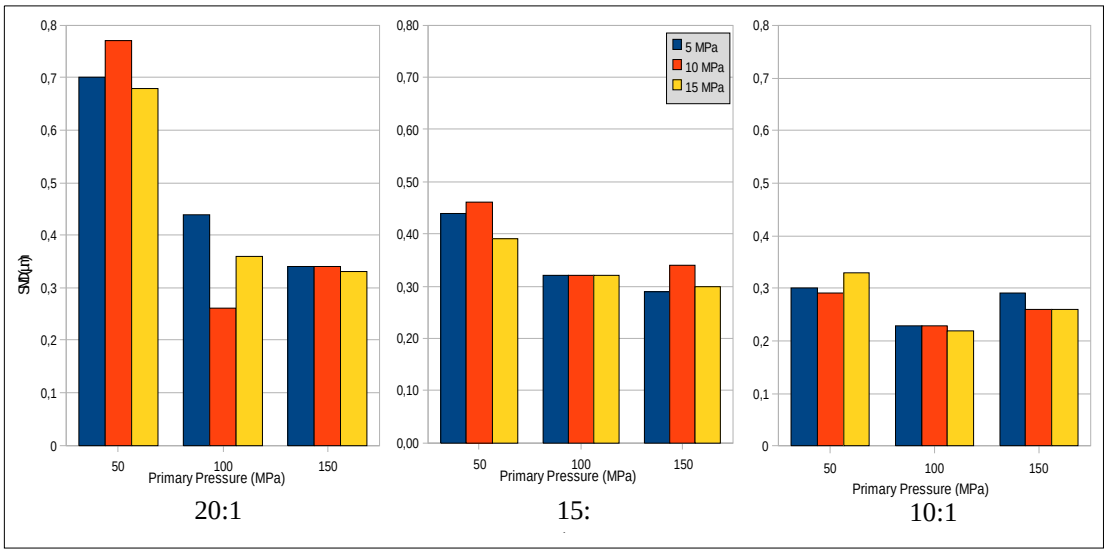


Figure 2.1: Sauter Mean Diameter of the three emulsion formulations homogenized at 50, 100 and 150 MPa as primary pressures. For each primary pressure, there are three different secondary pressures of homogenization, represented in the same stack.

The smallest diameters were obtained in the 10:1 formulation. Despite of a small tendency for smaller particles to be associated with higher primary pressure of homogenization, there is no relevant difference. Different secondary process pressures do not show any relevant change in droplet mean diameter.

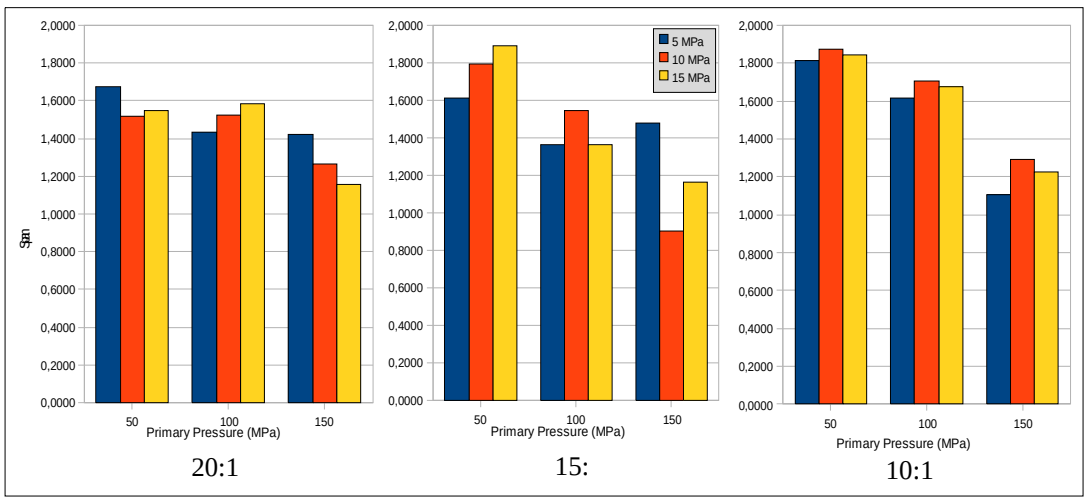


Figure 2.2: Distribution span of the three emulsion formulations, homogenized under 50, 100 and 150 MPa as primary pressures. For each primary pressure, three different secondary pressures of homogenization were applied, and are represented in the same stack.

The emulsions that were homogenized with a primary pressure of 150 MPa showed the narrowest particle distributions. Like in the particle diameter test, secondary process pressure showed little influence in distribution span.

### 2.2.2. Structural Stability Analysis

Similarly to the emulsions' droplet size determination, the structural stability was inspected by monitoring eventual changes of average droplet diameter and distribution width. Figure 2.3 shows the variation of the SMD of the three different formulations over time, and the variation of the droplet distribution span is shown in Figure 2.4. From observation of the plots, it is clear that mean droplet diameter and distribution span don't show any relevant variation over time.

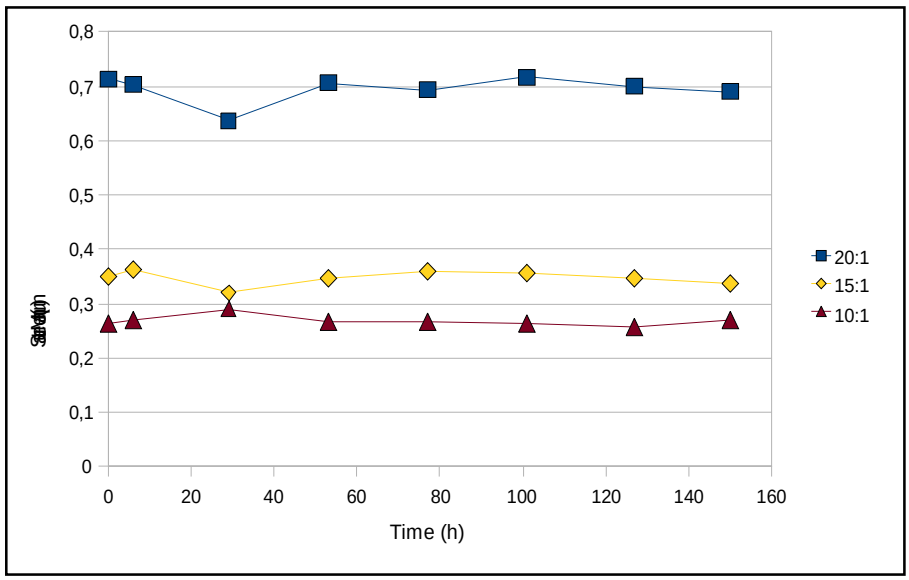


Figure 2.3: Variation of the Sauter Mean Diameter over time, for the three different emulsion formulations, homogenized under the same conditions.

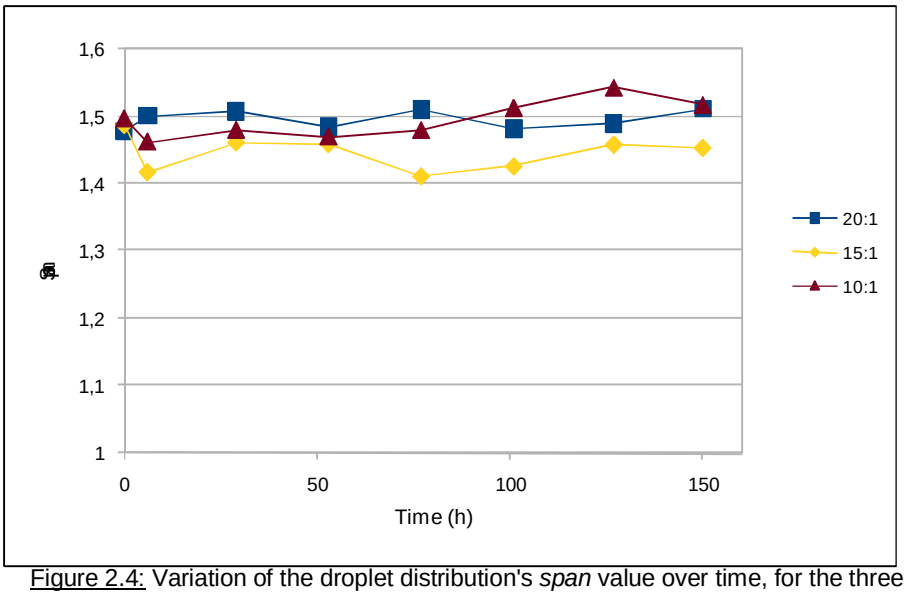


Figure 2.4: Variation of the droplet distribution's *span* value over time, for the three different emulsion formulations, homogenized under the same conditions.

### 2.2.3. Spectrophotometric Method

Using the spectrophotometer software for analysing the absorbance profile of β-carotene, it was found that maximum radiation is absorbed at a wavelength of 450nm (Figure 2.5). This wavelength was used to determine the relation between carotene concentration and absorbance. The calibration curve obtained from the linear region of the experimental points is shown in Figure 2.6. This calibration curve was adopted in the quantitative analysis of carotene on the homogenized emulsion and spray-dried powder.

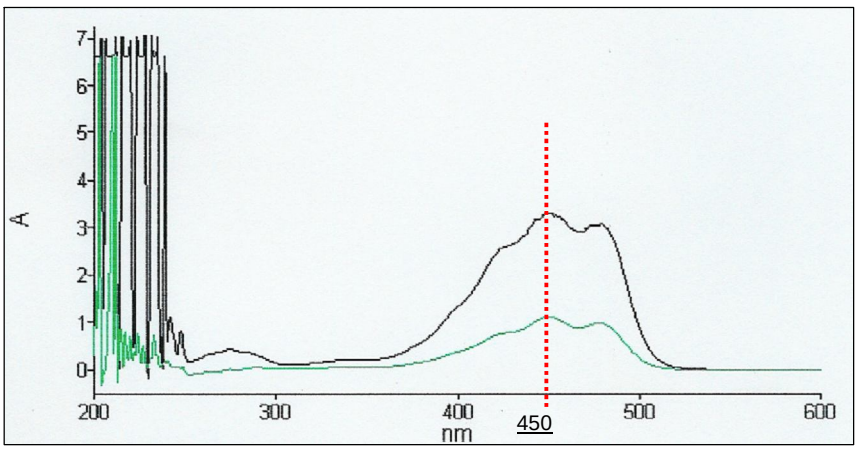


Figure 2.5: Absorbance profile of β-carotene, determined on two samples of different concentrations, showing a clear peak at 450nm.

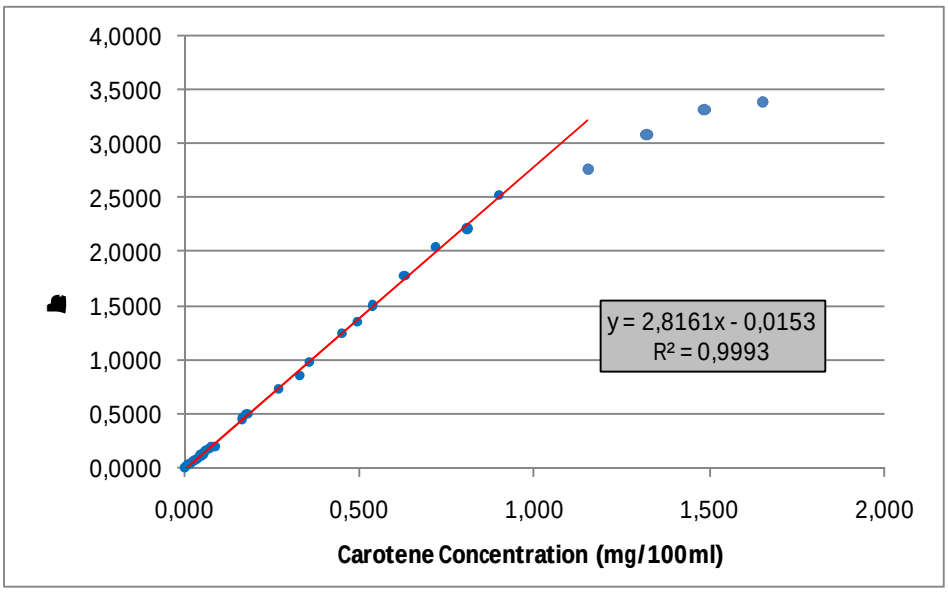


Figure 2.6: Calibration curve of β-carotene in hexane, at 450nm, with its correspondent regression equation.

### 2.2.4. Carotene Stability on Homogenization

Results shown in Figure 2.7 represent the loss of carotene on homogenization, related to the carotene content of the pre-mixed sample. It is clear that homogenization of the emulsion with a primary pressure of 50 MPa provides less destruction of carotene. The other pressures used show a higher loss, with no practical difference between them.

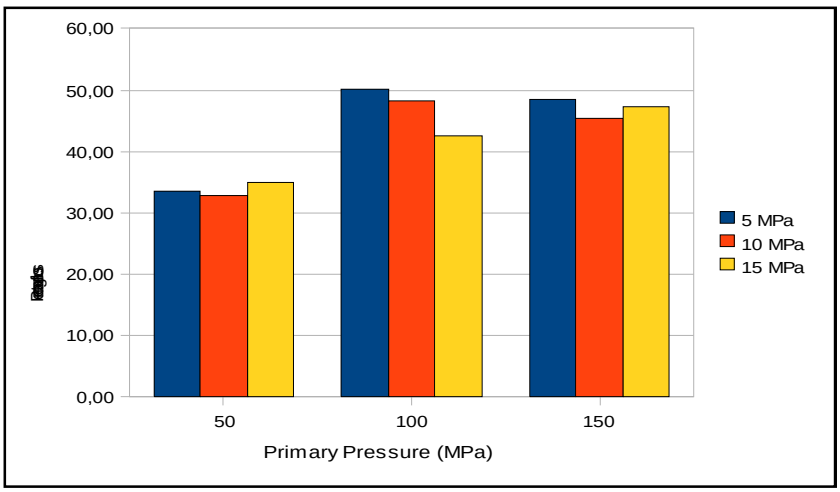


Figure 2.7: Percentage of carotene lost during homogenization, using the pre-mixed emulsion as reference. Results are shown for each combination of primary and secondary pressures.

# CHAPTER III – ENCAPSULATION: WATER SORPTION AND PHYSICAL STABILITY

The second part of the study is based on the emulsion produced according to the emulsion formulation and homogenization parameters optimized in the previous chapter. The selected feed emulsion had a formulation of 10:1 oil-to-protein ratio, was homogenized with 150MPa and 10MPa as primary and secondary process pressures, respectively. After spray-drying of the emulsion, the sorption behaviour of the matrix is studied, to relate with eventual crystallization. The effects of crystallization on the stability of the encapsulate and retention of the core material is then observed as the variation of the surface extractable oil, and the droplet distribution profile of the reconstituted emulsion. A microscopic observation of the powder is also conducted, to observe crystalline structures, under polarizing light. Further ahead, the thermal transitions of the lactose-trehalose sugar system are determined by DSC, to establish a relation with the crystallization phenomenon, and other methods for determination of the transitions are studied, such as DMA and DEA.

## 3.1. Materials and Methods

### 3.1.1. Production of the Spray-Dried Encapsulate

The emulsion selected according to the results of the preliminary study (Chap.II) was produced in a larger amount, with an approximate carotene concentration in oil of 0.8mg/g. The bulk emulsion was fed to a pilot plant scale spray-drier (Niro Atomizer, Denmark), set to an inlet temperature of 170ºC and an outlet temperature of 60ºC. Atomizer rotation speed was set to 22000rpm.

### 3.1.2. Determination of Sorption Isotherms

The spray-dried powder was distributed among small vials, which were in turn put in seven different desiccators, subject to different relative vapour pressures (RVP). The different relative vapour pressures were regulated by saturated solutions of different salts, due to their water activity. The relation between the aimed relative vapour pressure and the salt used is given in Table 3.1. All salts were supplied by Sigma-Aldrich.

Table 3.1: Relation between the theoretical water activities used (25ºC), and the salts that were placed as saturated solutions inside the desiccators.

| Water Activity | Salt |
|---|---|
| 0,11 | LiCl |
| 0,23 | $CH_3COOK$ |
| 0,33 | $MgCl_2$ |
| 0,44 | $K_2CO_3$ |
| 0,54 | $Mg(NO_3)_2$ |
| 0,65 | $NaNO_2$ |
| 0,76 | NaCl |

The desiccators were kept closed and under vacuum. Triplicate samples were collected to determine the weight variations of the powders. Knowing that the laboratory had a approximately constant temperature of 22ºC, constantly monitored, the water sorption data was used to plot an isotherm, based on the equilibrium water content of the powder for each water activity. The $a_w$ of the saturated salt solutions used was checked using an Aqualab CX-2 instrument, and results were corrected accordingly.

### 3.1.3. Encapsulation and Surface Oil Determination Over Hydration

Samples were kept in open glass vials under four different water activities, which were 0, 0.11, 0.33 and 0.54. The $a_w$ of 0 was accomplished with dry $P_2O_5$ (supplied by Sigma-Aldrich), instead of a solution, whereas the other three water activities were obtained as described before. The vials were stored under these conditions for a period of six weeks, and triplicate samples were regularly collected.

Total carotene in powder was determined by a method somewhat similar to the one used for carotene determination on emulsions (Chap.II). Firstly, about 1g (known mass, precise up to 0.01g) of powder was rehydrated with 5,00ml of distilled water. After gentle shaking, allowing the powder to dissolve, a mass of about 1g (precisely known) was further dispersed with roughly 8ml of distilled water. Afterwards, 5,00ml of hexane was added, and the mixture was manually shaken for 30 seconds in a plastic, screw-cap tube, to avoid evaporation of solvent. The hexane phase was then separated by centrifugation for 15 minutes at 2000rpm, and analysed by spectrophotometry.

Surface carotene was determined by washing about 0.5g (precisely known) of powder with 10,00ml of hexane. The mixture was made in the same kind of plastic, screw-cap tubes, which were constantly tilted to allow contact between the powder and the solvent. Both phases were separated by centrifugation at 2000rpm during 15 minutes, and the hexane was analysed by spectrophotometry.

### 3.1.4. Reconstituted Emulsion Structure

The emulsion resulting from re-dissolution of the powder in water was analysed for droplet size distribution over time. The emulsion used for this analysis was the same intermediate emulsion obtained when determining the total encapsulated carotene on the spray-dried powder. Droplet size was measured using laser diffractometry. This study was conducted alongside with the carotene determinations, also regularly for a period of six weeks.

### 3.1.5. Crystallization Detection by Microscopy

Microscopic observation was made on samples of the spray-dried powder, hydrated at 0%, 11%, 33% and 54% of relative humidity for seven days at least. The microscope used was a BX51 model by Olympus, provided with a light polarizer, and connected to a computer via a PixeLINK PL-A662 digital camera. For each sample, various snapshots were taken, allowing to compare the actual view with the view obtained by polarized light, thus detecting occurrence of crystallization. The powder was spread over a glass slide, where it remained uncovered, and observations were made at room temperature.

### 3.1.6. Determination of the Thermal Transitions

Thermal transitions were determined on amorphous sugar systems, intended to represent the carbohydrate matrix of the encapsulate. The sugar systems were prepared from a solution, with a solids content of 20% (w/w), of equal parts of lactose and trehalose. This is the same total solids content of the model emulsion, but in this study the protein is not included. The solution was prepared under heating, to aid dissolution, and then it was distributed into several Petri dishes. Afterwards the dished were put in a freezer for 24h at a

temperature of -20ºC, followed by another 48h period at -80ºC. Finally, the solution was dried in a freeze-drier (STERIS Lyovac GT2) for 48h, at a temperature of -40ºC and a pressure no higher than $10^{-2}$ mbar.

After drying, the sugar system was ground with a mortar and a pestle, and was distributed into small vials. The vials were stored into four different desiccators, under four different water activities, for at least 72 hours. The four different storage conditions were the same used for the previously referred carotene content study (0, 0.11, 0.33 and 0.54).

After ensuring proper hydration of the sugar systems, thermal transitions of the four different samples were determined by differential scanning calorimetry (DSC821e, Mettler Toledo, Switzerland). Samples were put in 40 µL aluminium pans, with an empty pan used as reference. The reference pan was pierced to allow evaporation, thus eliminating any influence of the water. The pan for the dehydrated sample ($a_w$=0.00) was also pierced, to ensure minimum moisture.

The DSC analysis was done in three stages, or temperature scans. The first two temperature scans consisted in bringing the temperature upwards and then downwards to the original value. This procedure has the effect of dissipating the energy absorbed by the system during the storage period in the desiccators. The third scan was the only meant to provide the actual data, and the thermogram obtained was analysed with the STARe 6.0 (Mettler Toledo) software, to determine the glass transition temperature, and crystallization temperature when possible. All temperature scans were made with a heating ratio of 5ºC/min and a cooling ratio of 10ºC/min. All samples were run in triplicate, and the scan range temperatures were adjusted between replications of the same sample, whenever necessary.

Analysis for the mechanical properties of the sugar system was made in a DMA instrument (Triton Technology Ltd.). Readings for the loss modulus and tanδ were collected during a temperature scan, using multiple frequencies of deformation, which were 0.5, 1.0, 5.0, 10.0 and 20.0 Hz. A steel pocket was used as a sample holder. Samples were cooled to the starting temperature using liquid nitrogen. Data was collected in a single run, and all samples were

run in triplicate, which allowed the temperature range of the scan to be corrected whenever necessary. All temperature scans were made with a heating ratio of 3ºC/min.

Analysis for the dielectrical properties of the sugar system was made in a DETA instrument (Triton Technology Ltd.). Readings for electrical permittivity and capacitance were collected during a temperature scan, using multiple frequencies of deformation, namely 0.5, 1.0, 5.0, 10.0 and 20.0 kHz. The sample was presented as a thin layer of powder, pressed between two parallel plate aluminium electrodes. The samples were cooled to the starting temperature using liquid nitrogen. Data was collected in a single run, and all samples were run in triplicate, which allowed the temperature range of the scan to be corrected whenever necessary. All temperature scans were made with a heating ratio of 3ºC/min.

## 3.2. Results

### 3.2.1. Determination of Sorption Isotherms

Results of water adsorption behaviour on the spray-dried powder over time, i.e. the variation of the moisture content, are shown in Figure 3.1. During the water sorption study, a moisture curve breakdown was observed on the samples hydrated under 76%, 65% and 54% RVP. This breakdown evidences water release, due to crystallization of the amorphous matrix. The $a_w$ values were corrected according to Table 3.2, based on measuring done on the salt solutions.

Table 3.2: Relation between the expected and the determined $a_w$, used for data correction.

| | | | | | | | |
|---|---|---|---|---|---|---|---|
| **Expected $a_w$** | 0,110 | 0,230 | 0,330 | 0,440 | 0,540 | 0,650 | 0,760 |
| **Determined $a_w$** | 0,127 | 0,232 | 0,339 | 0,451 | 0,592 | 0,664 | 0,781 |

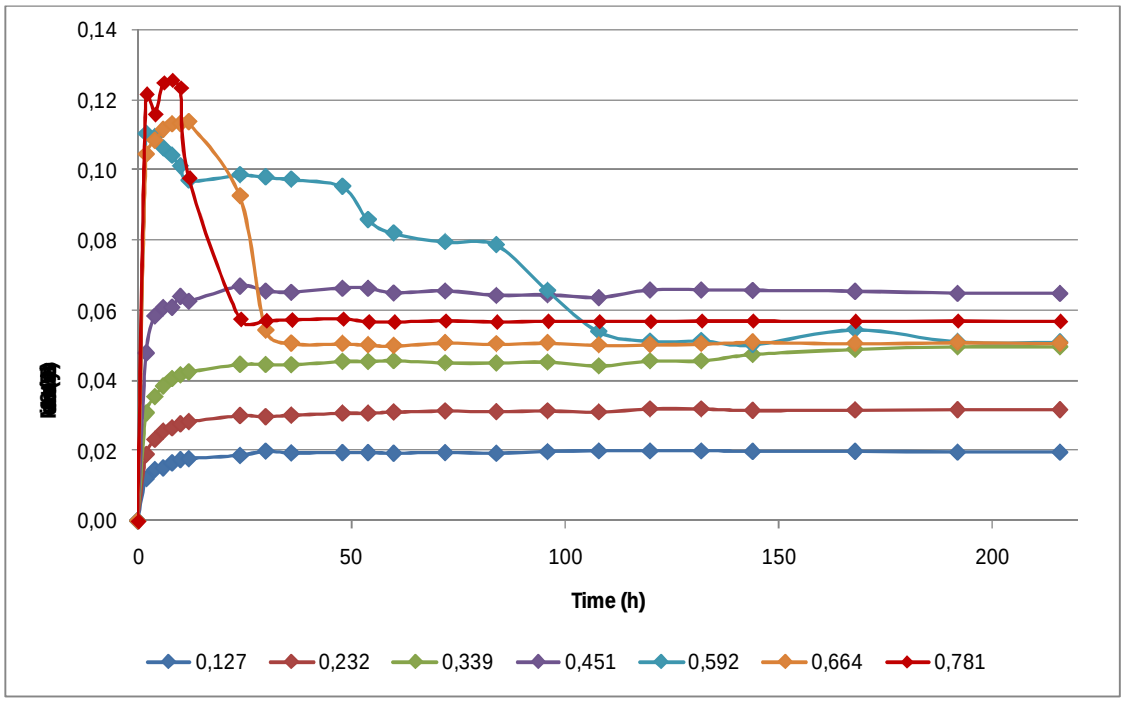


Figure 3.1: Water adsorption data for the spray-dried encapsulate, under the seven different water activities studied.

Considering the three samples that have crystallized, the 59,2% RVP environment took much longer than the other two. This is evidenced by the time necessary for the sorption curve to assume a constant value.

The equilibrium data obtained from Figure 3.1 allowed the determination of the sorption isotherm, as shown in Figure 3.2. Samples hydrated at water activities of 0.592, 0.664 and 0.781 show evidence of crystallization, and are considered inadequate for sorption studies.

The BET isotherm was adjusted using the linear form of the equation (see Literature Review, Eq. 1.1), which was computed in a spreadsheet software. The GAB sorption model was adjusted by second-order polynomial regression of Equation 1.2 (Literature Review) using the same software. Both isotherms are plotted over the experimental data in Figure 3.2.

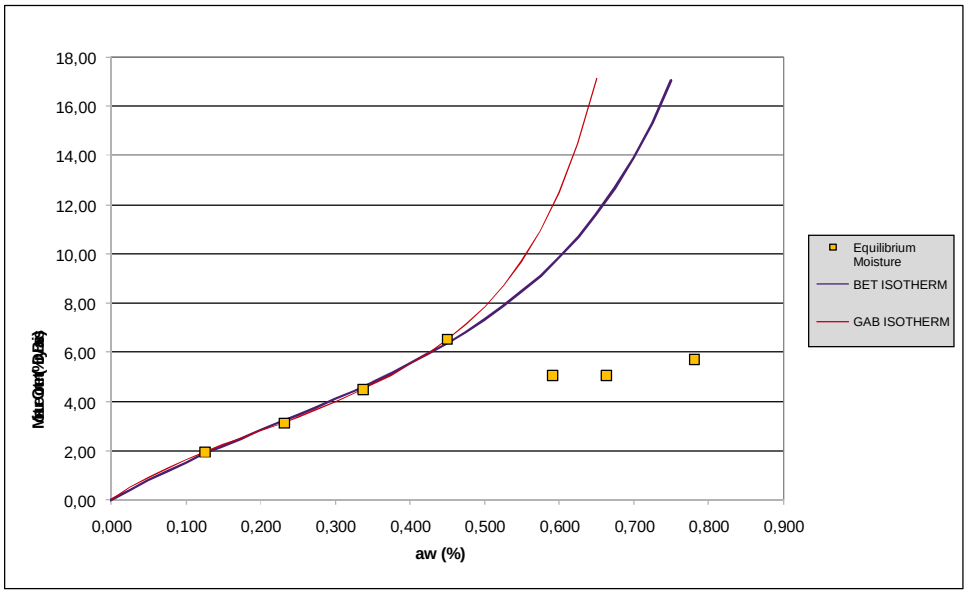


Figure 3.2: Water sorption isotherms at 25ºC of lactose-trehalose-sodium caseinate spray dried powder. Fitted and non-fitted experimental data are represented.

The parameters derived from the isotherms fitting are represented in Table 3.3. The relative percentage root mean square (%RMS) was calculated for both isotherms, as a measure for data fitting to the models. It should be noted that both the K constant of the BET model and the K' constant of the GAB model have no physical meaning and no correlation between them.

Table 3.3: Derived parameters of the fitted sorption isotherms. Parameter $m_1$ is in % moisture in dry basis, all other constants are dimensionless.

| **BET Isotherm** | | **GAB Isotherm** | |
|---|---|---|---|
| $\mathbf{m_1}$ | 4,638 | $\mathbf{m_1}$ | 3,208 |
| **K** | 3,809 | **K'** | 0,018 |
| | | **C** | 1,261 |
| **% RMS** | 2,758 | **% RMS** | 0,219 |

### 3.2.2. Encapsulation and Surface Oil Determination Over Hydration

Results of total encapsulated oil were inconsistent with any pattern, although they suggest that the amount of carotene in the powder remains constant for all samples, throughout the entire period of study. Surface oil results were far

more satisfactory, and they show a clear linear variation of the carotene content on the powder surface, slightly decreasing. This suggests that the experimental method used in determining total carotene content may not have been the most adequate, making the data unreliable, only providing indicative results. Both the total and surface oil plots are presented in the Appendix section, while the surface carotene as a fraction of the total content, is shown in Figure 3.3 for all water sorption assays.

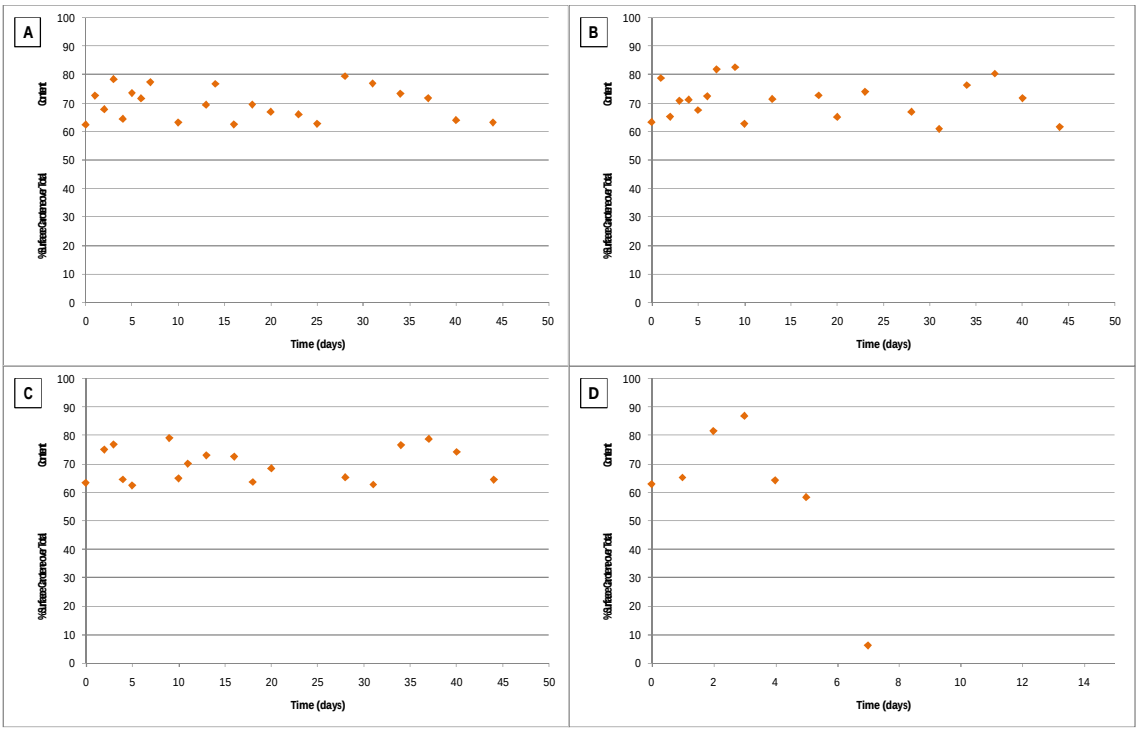


Figure 3.3: Variation of the surface carotene fraction over total carotene in the four storage $a_w$ values studied (A: 0.00; B: 0.127; C: 0.339; D: 0.592).

Regarding the sample hydrated under 59,2% RVP, determination of the surface carotene became impossible after day 8, due to caking of the powder, which formed one single clump, irreversibly affecting the surface of extraction. Nevertheless, the plot shows that this decrease of the total extractable carotene was gradual. Surface carotene proportion may have increased in the period of time before the sudden drop, but this is no more than a suggestion, due to the short period of time involved and the unreliability of the experimental method adopted.

### 3.2.3. Reconstituted Emulsion Structure

Droplet size distribution of the reconstituted emulsion was slightly different to that of the original emulsion which was fed to the spray-drier. This shows that the emulsion suffers slight changes during the spray-drying/reconstitution stage. The original emulsion was well homogenized, showing a unimodal distribution of droplet sizes, whereas the reconstituted emulsion showed a slight degree of re-coalescence, which generated a more relevant amount of particles over 1µm (Figure 3.4).

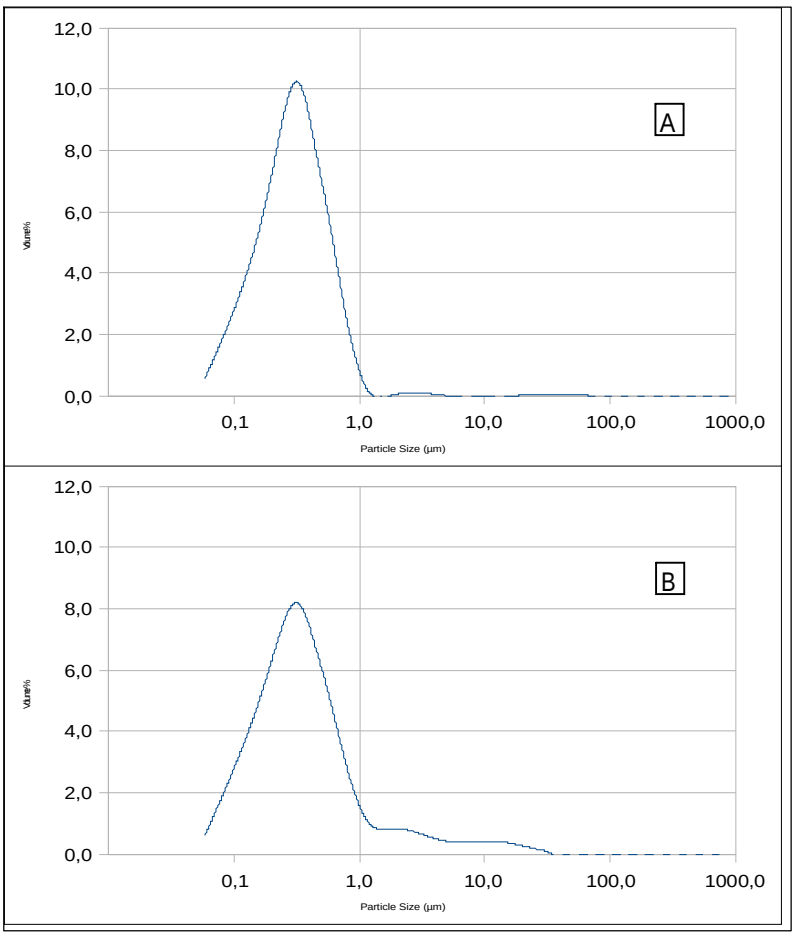


Figure 3.4: Comparison between droplet size distributions of the feed emulsion (A) and the emulsion resulting from rehydration of the encapsulate (B), on the same day of production.

Considering the powder stored under 0%, 12,7% and 33,9% RVP, the structure of the dispersed emulsion didn't suffer any change over time. In fact, both the mean droplet diameter and the distribution span didn't show evidence of variation, as shown in Figures 3.5 and 3.6. However, the powder stored under 59,2% RVP suffers a clear change in both parameters, from day 8

onwards. The increase in droplet diameter is somewhat regular, whereas the distribution span shows no regular variation, as it's related to the droplet re-coalescence phenomenon.

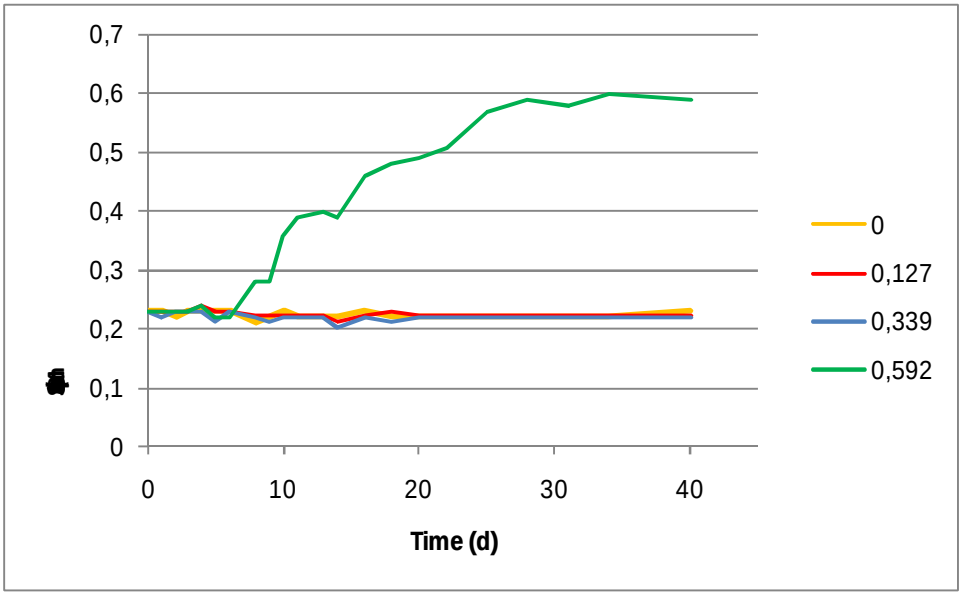


Figure 3.5: Variation over time of the Sauter Mean Diameter (D(3,2)) of the reconstituted emulsions of the four different powder samples.

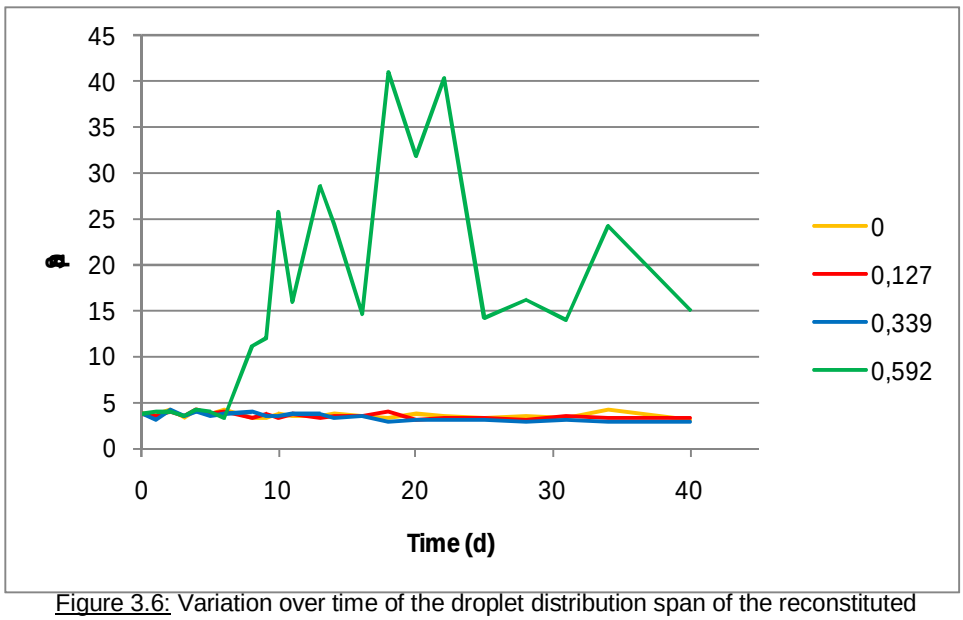


Figure 3.6: Variation over time of the droplet distribution span of the reconstituted emulsions of the four different powder samples.

A comparison of typical droplet distribution curves for the deviating sample (59,2% RVP) in different days is shown in Figure 3.7. It is clear that the curve gradually develops a multimodal shape of 3 peaks.

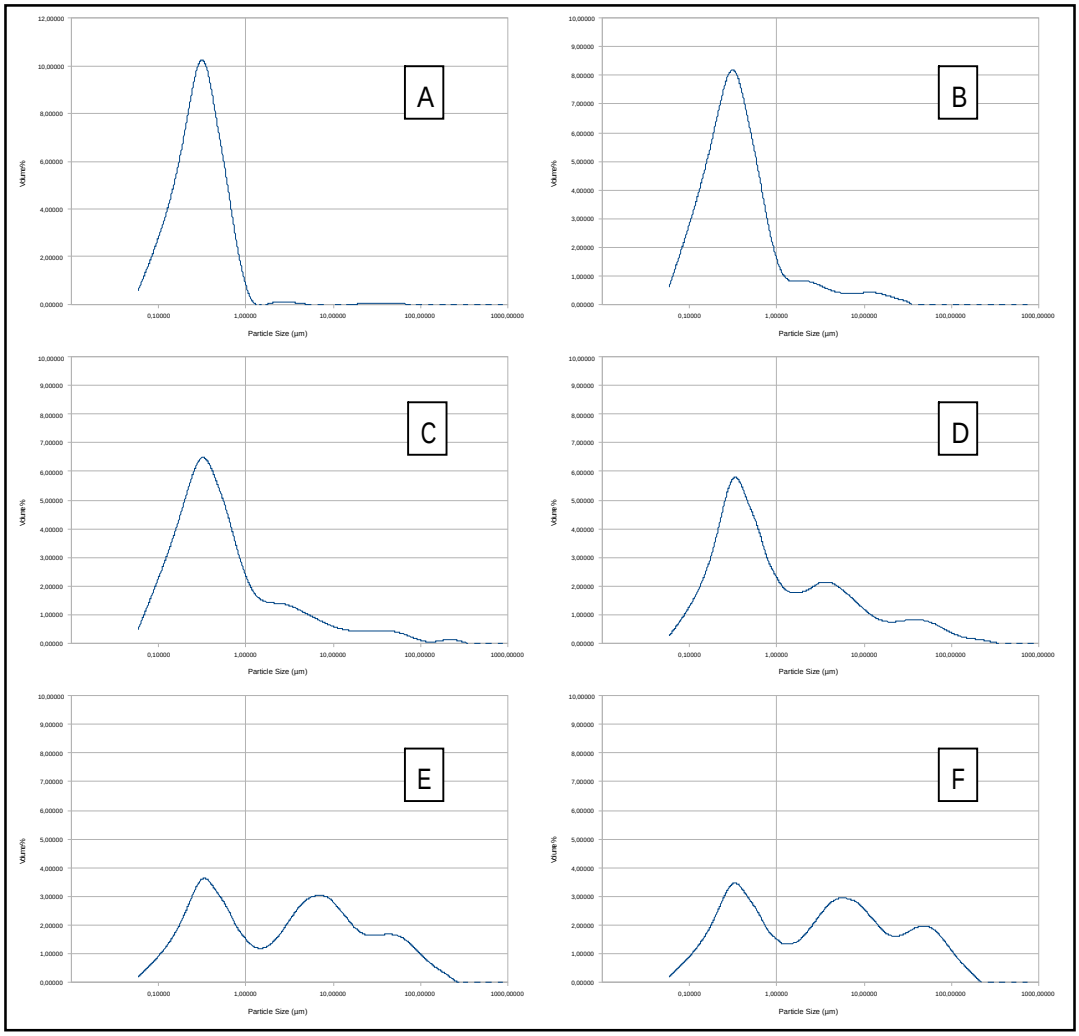


Figure 3.7: Comparative sequence of droplet size distribution curves of the reconstituted emulsion, resulting from rehydration of the powder at 59,2% RVP
(A: Original feed emulsion; B: Day 0; C: Day 9; D: Day 14; E: Day 25; F: Day 40).

### 3.2.4. Crystallization Detection by Microscopy

The spray-dried encapsulate was observed under the microscope at the end of the six weeks storage, under the four different relative vapour pressures. For the powders stored at 0%, 12,7% and 33,9% RVP, observations done with polarizing light showed nothing but a dark field, which indicates absence of crystals. Samples stored at 59,2% RVP showed clear crystallization, as shown in Figure 3.8.

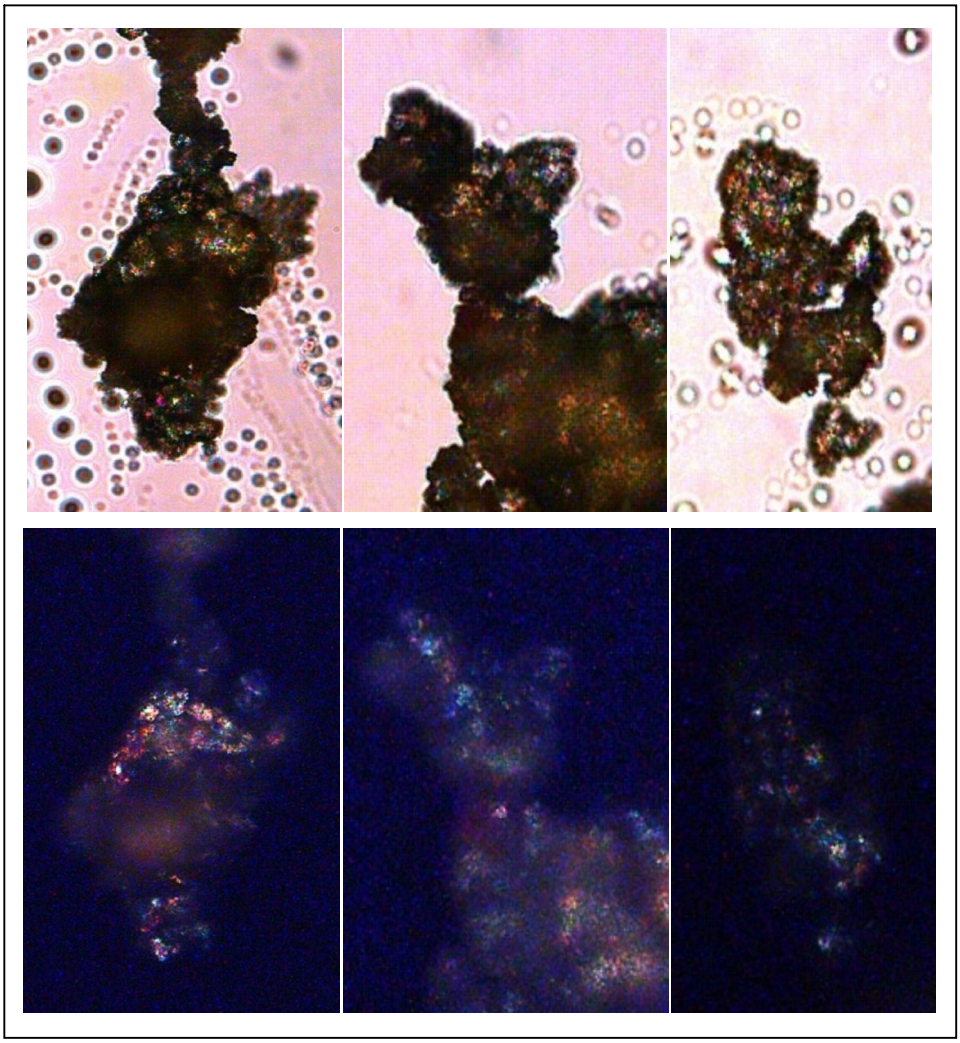

Figure 3.8: Comparison of details of microscopic snapshots taken from the powder, hydrated under 59,2% RVP. Upper snapshots were lit with regular white light and lower snapshots were taken under polarizing light, evidencing crystalline structures (magnification= 20X).

### 3.2.5. Determination of the Thermal Transitions

The sugar system hydrated under 59,2% RVP lost its powder form and became a clump. It was not subjected to any further analysis, since the loss of structure was already obvious for the time of storage.

For glass transition determination by DSC, onset, midpoint and endset temperatures are presented (Table 3.4). Besides the glass transition, first-order transitions were also detected on the samples hydrated under 33,9% RVP, at temperatures ranging from 120 to 140ºC. These transitions

correspond to the instant crystallization temperatures, and were not analysed in detail.

Table 3.4: Glass transition temperatures (onset, midpoint and endset) determined by DSC on the lactose-trehalose sugar system.

| RVP (%) | $T_g$ | | |
|---|---|---|---|
| | Onset | Midpoint | Endset |
| 0,0 | 107,9 | 113,9 | 122,9 |
| 12,7 | 55,2 | 61,3 | 72,0 |
| 33,9 | 30,1 | 36,6 | 47,6 |

To correlate with glass transition data from DSC, the loss modulus (E'') peak was assessed from the DMA data. Such temperatures, as well as the respective frequencies of deformation, were used to plot Arrhenius functions. These are plots of the natural logarithm of frequency (*ln f*) against the reciprocal absolute temperature (*1/T*, in $K^{-1}$), and are represented in Figure 3.9.

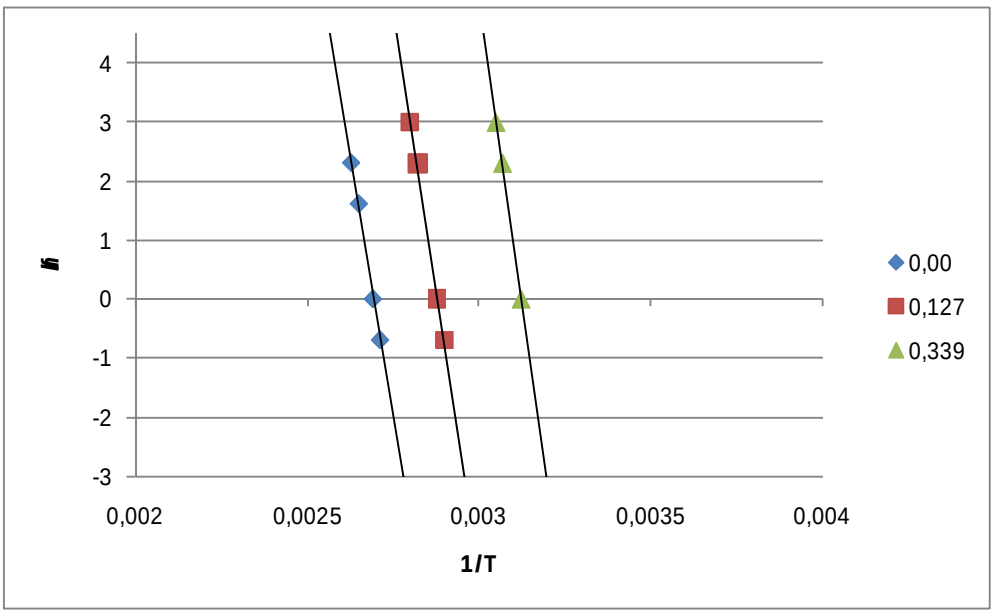


Figure 3.9: Arrhenius plots of the DMA results, showing the linear relation between frequency of deformation and E'' peak.

The purpose of these plots was to correlate the $T_g$ determined by DSC with a frequency of deformation used in mechanical analysis. However, the results obtained were considered as highly unreliable, due to little coherence between the triplicate analyses. This irregularity and unreliability is the reason why some of the experimental have been excluded, and not all 5 frequencies have been considered. Correlation coefficients of the linear data fitting were 0.9980 for the 0% RVP sample, 0.9965 for the 12,7% RVP, and 0.9990 for 33,9% RVP. It was found that in samples 12,7% and 33,9%, DMA analysis with a deformation frequency of about 0,015Hz could be correlated with the midpoint temperature of glass transition determined by DSC. However, the 0% sample could not be correlated. Full storage and loss modulus curves obtained by DMA are shown in the Appendix section.

As for the DEA analysis, *tan δ* peaks were very hard to obtain. In fact, the shape of the curves was very different than expected, showing an abrupt increase at high temperatures (above 100ºC). Most of the data collected from the curves resulted from a "suggested" peak, detected around the same temperature where the di-electrical constant (ε') breaks down. However, such peaks are also inaccurate, due to small resolution, i.e. a larger amount of experimental points in the peak area would provide greater accuracy. Full di-electric constant and *tan δ* curves obtained by DEA are shown in the Appendix section.

## CHAPTER IV – GENERAL DISCUSSION AND CONCLUSIONS

### 4.1. General Discussion

Emulsion formulation and homogenization parameters were selected according to mean droplet diameter, distribution width, emulsion structural stability and degree of carotene destruction in the homogenization process.

Smaller droplet diameter was mainly favoured by higher concentrations of sodium caseinate, whereas a smaller distribution width is favoured by a high pressure of homogenization, especially on the primary process. It is suggested than the influence of a higher homogenization pressure is enhanced by a higher concentration of emulsifier.

Loss of carotene in the homogenization process was significantly smaller when 50 MPa of primary pressure was used. Although higher, there was no significant difference between carotene degradation when 100 or 150 MPa was used. All samples have shown a very similar and acceptable structural stability, both in mean droplet diameter and span, over the period of time considered.

Therefore, considering that best encapsulate protection and efficiency is ensured by smaller droplet sizes, the highest emulsifier concentration and primary homogenization pressure were selected, i.e. a 10:1 oil:protein emulsion was homogenized with 150 MPa as primary pressure. Secondary pressure showed no significant influence in both the emulsion and the carotene content, within the same primary pressure used, so the middle value of 10 MPa was selected.

Sorption study shows that samples stored under relative vapour pressures of 78,1%, 66,4% and 59,2% crystallize spontaneously after a short period of time. However, the time necessary for the 59,2% RVP sample to crystallize was significantly longer, which shows the influence of the hydration speed on the crystallization speed.

The GAB sorption model provided a much smaller %RMS figure, which means it represents a better fit to the experimental data than the BET model. Theoretically, the GAB model would provide a better description of sorption data above $a_w$ values of 0.5. However, such $a_w$ levels were associated with quick crystallization of the matrix at

room temperature (22ºC), and could not be assessed Determined monolayer moisture values ($m_1$) were 4,64% and 3,21%, when determined by the BET and GAB models, respectively. These figures are consistent with the results of Omar and Roos (2007a) and Karel (1975, *cit. in* Lewis, 1996).

Total carotene content suffered no apparent change over the time dedicated to this study. In fact, the stored powder was stored away from light and oxygen, in hermetically sealed desiccators. Therefore, oxidation of carotene would only be possible by auto-oxidation, which would take a minimum of 4 to 6 weeks to produce any noticeable degradation of carotene (Rodríguez-Hueso *et al*, 2004). Furthermore, the adopted method for carotene extraction from the emulsion has proved to be unreliable. Anyway, great interest was put in the fraction of the total carotene that was exposed on the powder's surface. This parameter shows no variation over time for samples stored under 12,7% and 33,9% RVP. As for the 59,2% RVP sample, collapse of the matrix might have caused release of oil from the matrix, but the associated caking phenomenon reduces the powder's available surface for extraction, with inevitable reduction of the amount of extractable oil to nearly zero.

In comparison with the original emulsions, reconstituted emulsions show some re-coalescence, which creates some particles of sizes above 1µm. Nevertheless, the particle size profile remains constant for the rest of the period of study. This means that the emulsion is not necessarily unstable, but perhaps the shear forces in the spray-dryer's nozzle have been responsible for the structure changes of the emulsion. Eventually, the rehydration process could also have been responsible for some recoalescence. To inspect this possibility, it could be useful to determine the oil droplet size on the dry emulsion, by microscopic analysis.

Considering the four hydration environments tested, only the powder stored under 59,2% RVP showed structural changes on its reconstituted emulsion. The increased droplet mean diameter and distribution width shows that the collapse of the matrix structure caused re-coalescence of the oil droplets. This may be influenced by the slower dissolution of the crystalline matrix in water, which separates from the other constituents of the powder, including some remaining amorphous matrix. The dispersed phase of the emulsion was food-grade sunflower oil, which is liquid at room temperature; this may not have been beneficial for the integrity of the spray-dried powder, as the oil flows more easily than a solid lipid would.

Glass transition temperatures determined by DSC are slightly higher than of pure lactose and pure trehalose in the anhydrous sample. However, samples hydrated with higher humidities showed equal or lower values of Tg than those of the pure constituents (Elizalde et al, 2002, Roos and Karel, 1991). showed consistent results with literature, and replicates support the reliability of the data. This could not be achieved by DMA and DEA analysis. In DMA analysis, the possible correlation with the DSC results was found at a very low frequency – 0,015Hz - but such results were not sufficiently supported by the experimental data, as many results were deemed incoherent.

In most samples, results obtained by DEA gave nothing that could be interpreted as the glass transition as the results were, like the DMA results, very inconsistent. However, the DSC correlation frequencies provided by the sample kept under 0% RVP presented a distinct order of values than of the other two samples.

Considering the moisture dependent nature of the thermal transitions, it must be noted that both the DMA and DEA instruments don't limit the evaporation of water during the heating up cycles. DSC analysis controls this problem, since samples are heated inside small, hermetically sealed pans, which aim to avoid evaporation of water, thus minimizing deviations to the glass transition temperatures obtained. In DMA and DEA, sample holders were open, although they were put in closed cells. Therefore, detection of $T_g$ with such methods may be inadequate when the temperatures are situated above the evaporation point of water, since loss of water changes the properties that were to be detected. It should be noted that the samples which were stored under 0% RVP showed more characteristic shapes of curves, both in mechanical and di-electrical properties, which may suggest a relation between unpredictable data and the existence of moisture in the samples.

Furthermore, the more uncharacteristic behaviour of the DEA may be related to the higher influence of water in dielectric than in mechanical properties, or the frequencies set for the analysis were too high. It is also suggested that small molecular weight carbohydrates may show different mechanical behaviour, especially when hydrated, which may create difficulties that don't exist in more mechanical sensitive materials, like polymeric substances.

Crystallization of the spray-dried powder stored under 59,2% RVP is well observed by microscopic observation, using polarizing light. Microscopic data has also shown that the collapse of the powder structure favours droplet re-coalescence.

### 4.2. Conclusions

Overall, it can be concluded that encapsulation matrices of amorphous lactose-trehalose systems remain stable if kept at an $a_w$ of 0.451 and below, for the time range considered in this study. Higher humidities during storage result in crystallization of the matrix after a short period of time, which leads to collapse of the powder's structure. This event strongly reduces the powder's flowability, barrier effect and ability to rehydrate into the original emulsion.

High-pressure homogenization has proved to be a good method to reduce droplet size in a oil-in-water emulsion. The emulsions obtained were physically stable for an acceptable time period. However, the secondary homogenization process has shown no visible advantage, for the emulsion formulations considered.

DSC analysis shows onset glass transition temperatures of 107,9ºC for 0% RVP storage, 55,2ºC for 12,7% RVP and 30,1ºC for 33,9% RVP, which were similar to the values expected in the literature. This shows a great difference between hydrated and non-hydrated amorphous sugars, in terms of the glass transition, evidencing the possibility of dropping the $T_g$ to room temperature, if the storage humidity is not kept under control.

Correlation between DSC results and the ones obtained by DMA and DEA was not possible, due to very irregular data returned. However, a correlation frequency of 0.015Hz was found for samples hydrated under 12,7% and 33,9% RVP. No indicative values were obtainable by DEA. Crystallization of the matrix was successfully detected by microscopic observation, on the sample hydrated under 59,2% RVP.

Extraction of carotene from emulsions is incomplete and irregular if done as a simple contact with hexane. A more complex extraction method would be more reliable, but maybe unnecessary due to the nature of this project and the level of detail required for the results.

Adsorption behaviour of the model sugar system has been fitted to the BET and GAB sorption models, and monolayer moisture contents (dry basis) have been determined as 4,64% and 3,21% for BET and GAB isotherms, respectively. These values are acceptable, within other values reported.

It is concluded that the production of encapsulates from oil-in-water emulsions can be benefitted if ultra-high pressure homogenization is used to reduce mean droplet size. The lactose-trehalose matrix offers good physical stability as an encapsulation matrix. However, a more thorough study on the efficiency of encapsulation is needed, using better experimental methods, so that reliable quantitative data can support this work. Also the mechanical and di-electrical methods for thermal transition determination must be adjusted to the characteristics of the sample to develop a reliable correlation with the DSC results.

## REFERENCES


Baranauskienė, R.; Venskutonis, P.R.; Dewettinck, K.; Verhé, R. **(2005)**. Properties of oregano (*Origanum vulgare* L.), citronella (*Cymbopogon nardus* G.) and marjoram (*Majorana hortensis,* L.) flavors encapsulated into milk protein-based matrices. *Food Research International*, 39: 413-425.

Bhandari, B.R.; D'Arcy, B.R.; Padukka, I. **(1999)**. Encapsulation of Lemon Oil by Paste Method Using β-Cyclodextrin: Encapsulation Efficiency and Profile of Oil Volatiles. *Journal of Agricultural and Food Chemistry*, 47: 5194-5197.

Campos, L. **(2002)**. *Entender a Bioquímica*. 3ª Edição. Escolar Editora, Lisboa, Portugal.

Christensen, K.L.; Pedersen, G.P.; Kristensen, H.G. **(2001)** Preparation of redispersible dry emulsions by spray-drying. *International Journal of Pharmaceutics,* 212: 187-194.

Deladino, L.; Anbinder, P.S.; Navarro, A.S.; Martino, M.N. **(2006)**. Co-crystallization of yerba mate extract (*Ilex paraguariensis*) and mineral salts within a sucrose matrix. *Journal of Food Engineering*, 80: 573-580.

Duarte, C.S.C. **(2006)**. *Encapsulamento de aroma de alho em matriz de amido. Utilização dos encapsulados em panificação*. Relatório Final de Curso da Licenciatura em Engenharia Alimentar. Instituto Superior de Agronomia/Universidade Técnica de Lisboa. Lisboa, Portugal.

Elizalde, B.E.; Herrera, M.L; Buera, M.P. **(2002)** Retention of β-Carotene Encapsulated in a Trehalose-based Matrix as Affected by Water Content and Sugar Crystallization. *Journal of Food Science*, 67 (8): 3039-3045

Fuchs, M.; Turchiuli, C.; Bohin, M.; Cuvelier, M.E.; Ordonnaud, C.; Peyrat-Maillard, M.N.; Dumoulin, E. **(2005)**. Encapsulation of oil in powder using spray drying and fluidised bed agglomeration. *Journal of Food Engineering*, 75: 27-35.

Gibbs, B.F.; Kermasha, S.; Alli, I.; Mulligan, C.N. **(1999)**. Encapsulation in the food industry: a review. *International Journal of Food Sciences and Nutrition*, 50: 213-224.

Gouin, S. **(2003)**. Micro-encapsulation: industrial appraisal of existing technologies and trends. *Trends in Food Science & Technology*, 15: 330-347.

Gunning, Y.M.; Gunning, P.A.; Kemsley, E.K.; Parker, R.; Ring, S.G.; Wilson, R.H.; Blake, A. **(1999)**. Factors Affecting the Release of Flavor Encapsulated in Carbohydrate Matrixes. *Journal of Agricultural and Food Chemistry*, 47: 5198-5205.

Gunning, Y.M.; Parker, R.; Ring, S.G.; Rigby, N.M.; Wegg, B.; Blake, A. **(2000)**. Phase Behavior and Component Partitioning in Low Water Content Amorphous Carbohydrates and Their Potential Impact on Encapsulation of Flavors. *Journal of Agricultural and Food Chemistry*, 48: 395-399.

Guzey, D.; McClements, D.J. **(2006)**. Formation, stability and properties of multilayer emulsions for application in the food industry. *Advances in Colloid and Interface Science*, 128-130: 227-248.

Kaushik, V.; Roos, Y.H. **(2006)**. Limonene encapsulation in freeze-drying of gum Arabic-sucrose-gelatin systems. *LWT – Food Science and Technology*, 40 (8): 1381-1391.

Laaksonen, T.J.; Roos, Y.H. **(2000)** Thermal, Dynamic-mechanical, and Dielectric Analysis of Phase and State Transitions of Frozen Wheat Doughs. *Journal of Cereal Science*, 32: 281-292.

Levine, H.; Slade, L. **(1992)**. Glass Transitions in Foods. In: Schwartzberg, H.G.; Hartel, R.W.(ed.), *Physical Chemistry of Foods*, Chap.3. Marcel Dekker, Inc. New York, U.S.A. Chap. 3.

Lewis, M.J. **(1996)**. *Physical Properties of Food and Food Processing Systems*. Woodhead Pubslishing, Ltd. Cambridge, U.K.

Lievonen, S.M.; Roos, Y.H. **(2003)**. Comparison of dielectric properties and non-enzymatic browning kinetics around glass transition. *Innovative Food Science and Emerging Technologies*, 4, 297-305.

Madene, A.; Jacquot, M.; Scher, N.; Desobry, S. **(2006)**. Flavour encapsulation and controlled release – a review. *International Journal of Food Science and Technology*, 41: 1-21.

Minemoto, Y.; Adachi, S.; Matsuno, R. **(1997)**. Comparison of Oxidation of Methyl Linoleate Encapsulated with Gum Arabic by Hot-Air-Drying and Freeze-Drying. *Journal of Agricultural and Food Chemistry*, 45: 4530-4534.

Omar, A.M.E.; Roos, Y.H. **(2007a)**. Water sorption and time-dependent crystallization behaviour of freeze-dried lactose-salt mixtures. *LWT-Food Science and Technology*, 40: 520-528.

Omar, A.M.E.; Roos, Y.H. **(2007b)**. Glass transition and crystallization behaviour of freeze-dried lactose-salt mixtures. *LWT-Food Science and Technology*, 40: 536-543.

Pegg, R.B.; Shahidi, F. **(1999)**. Encapsulation and Controlled Release in Food Preservation. In Rahman, M.S. (ed.), *Handbook of Food Preservation*, Chap.21. Marcel Dekker, Inc. New York, U.S.A.

Reineccius, G.A. **(1994)**. Flavor Encapsulation. In Krochta, J.M. (ed.); Baldwin, E.A. (ed.); Nisperos-Carriedo, M.O., *Edible Coatings and Films to Improve Food Quality*. Technomic Publishing Co., Lancaster, U.S.A.

Rodríguez-Hueso, M.E.; Pedroza-Islas, R.; Prado-Barragán, L.A.; Beristain, C.I.; Vernon-Carter, E.J. **(2004)** Microencapsulation by Spray Drying of Multiple Emulsion Containing Carotenoids. *Journal of Food Science*, 69 (7): 351-359.

Roos, Y.H. **(1987)**. Effect of Moisture on the Thermal Behavior of Strawberries Studied using Differential Scanning Calorimetry. *Journal of Food Science*, 52 (1): 146-149.

Roos, Y.; Karel, M. **(1991)**. Plasticizing Effect of Water on Thermal Behavior and Crystallization of Amorphous Food Models. *Journal of Food Science*, 56 (1): 38-43.

Roos, Y.H. **(1992)**. Phase Transitions and Transformations in Food Systems. In: Heldman, D.R.; Lund, D.B., *Handbook of Food Engineering*. Chap.3, Marcel Dekker, Inc. New York, U.S.A. Chap. 3.

Roos, Y.H. **(1995)**. *Phase Transitions in Foods*. Academic Press. London, U.K. pp.19-47; 50-53; 86-97; 193-240; 247-262.

Soottitantawat, A.; Yoshii, H; Furuta, T.; Ohkawara, M.; Linko, P. **(2003)**. Microencapsulation by Spray Drying: Influence of Emulsion Size on the Retention of Volatile Compounds. *Journal of Food Science*, 68 (7): 2256-2262.

Soottitantawat, A.; Bigeard, F.; Yoshii, H.; Furuta, T.; Ohkawara, M.; Linko, P. **(2004)**. Influence of emulsion and powder size on the stability of encapsulated D-limonene by spray drying. *Innovative Food Science and Emerging Technologies*, *6: 107-114.*

Sutter, S.C.; Buera, M.P.; Elizalde, B.E. **(2007)**. β-Carotene encapsulation in a mannitol matrix as affected by divalent cations and phosphate anion. *International Journal of Pharmaceutics*, 332: 45-54.

Szente, L.; Szejtli, J. **(2003)**. Cyclodextrins as food ingredients. *Trends in Food Science and Technology.* 15: 137-142.

Talja, R.A.; Roos, Y.H. **(2001)** Phase and state transition effects on dielectric, mechanical, and thermal properties of polyols. *Termochimica Acta*, 380:109-121.

Turchiuli, C.; Fuchs, M.; Bohin, M.; Cuvelier, M.E.; Ordonnaud, C.; Peyrat-Maillard, M.N.; Dumoulin, E. **(2005)**. Oil encapsulation by spray drying and fluidised bed agglomeration. *Innovative Food Science and Emerging Technologies*, 6: 29-35.

Ubbink, J.; Krüger, J. **(2006)**. Physical approaches for the delivery of active ingredients in foods. *Trends in Food Science and Technology*, 17: 244-254.

Vega, C.; Roos, Y.H. **(2005)**. Invited Review: Spray-Dried Dairy and Dairy-Like Emulsions – Compositional Considerations. *Journal of Dairy Science*, 89: 383-401.

Vega, C.; Goff, H.D.; Roos, Y.H. **(2006)**. Casein molecular assembly affects the properties of milk fat emulsions encapsulated in lactose and trehalose matrices. *International Dairy Journal*, 17 (6): 683-695.

Vieira, S.I.C.D. **(1998)**. *Extracção e encapsulamento do aroma de Origanum vulgare L.* Relatório Final de Curso da Licenciatura em Engenharia Agro-Industrial. Instituto Superior de Agronomia/Universidade Técnica de Lisboa. Lisboa, Portugal.

Walstra, P. **(2003)**. *Physical Chemistry of Foods*. Marcel Dekker, Inc. New York, U.S.A. pp.250-281; 302-307; 583-591; 650-669.

Weiss, J.; Takhistov, P.; McClements, D.J. **(2006)**. Functional Materials in Food Nanotechnology. *Journal of Food Science*, 71 (9): 107-116.

## APPENDIX

A. **Total Carotene and Surface Carotene Plots Over Time.**

B. **Dynamic Mechanical Analysis (DMA) Results.**

C. **Di-Electrical Analysis (DEA) Results.**

## A. TOTAL CAROTENE AND SURFACE CAROTENE PLOTS OVER TIME

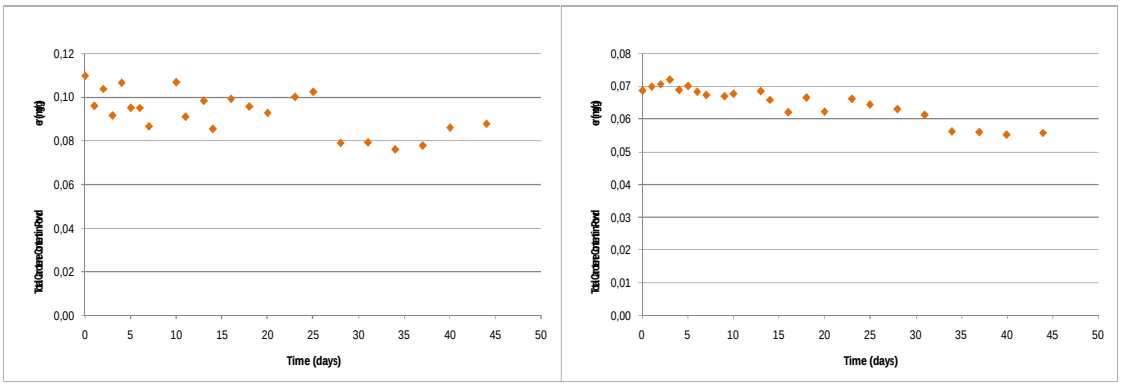


Figure A.1: Variation of the total carotene content (left) and surface carotene (right) of the encapsulate hydrated under an $a_w$ of 0,00.

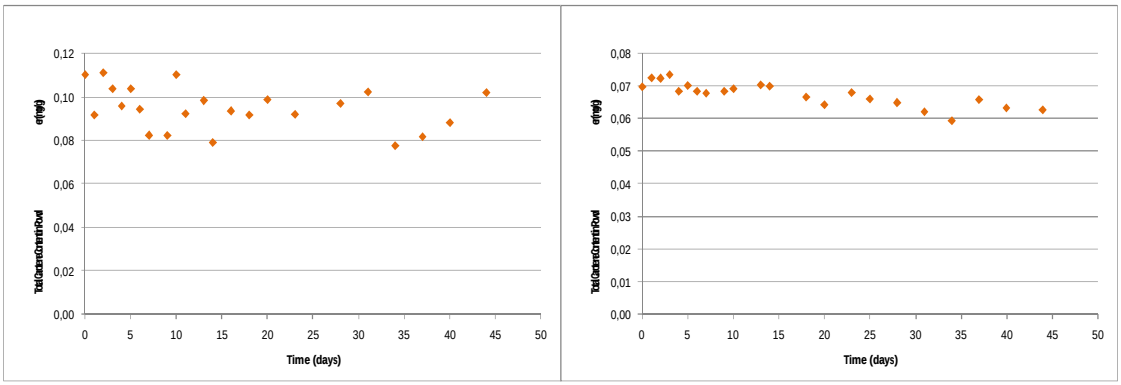


Figure A.2: Variation of the total carotene content (left) and surface carotene (right) of the encapsulate hydrated under an $a_w$ of 0,127.

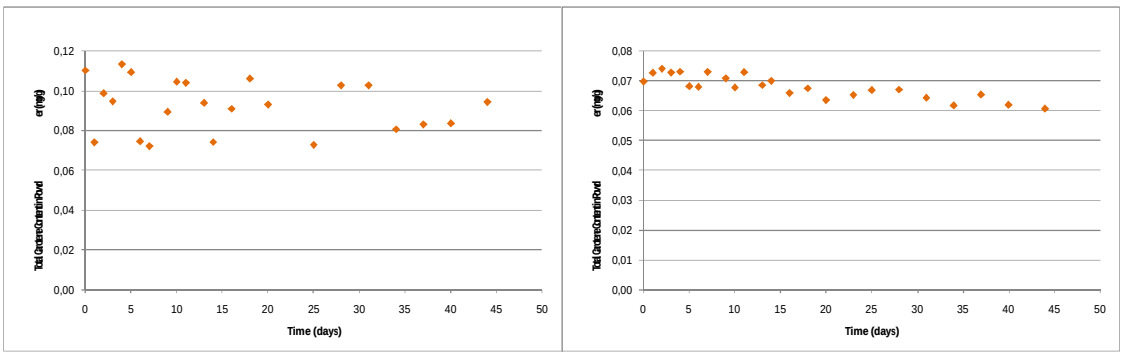


Figure A.3: Variation of the total carotene content (left) and surface carotene (right) of the encapsulate hydrated under an $a_w$ of 0,339.

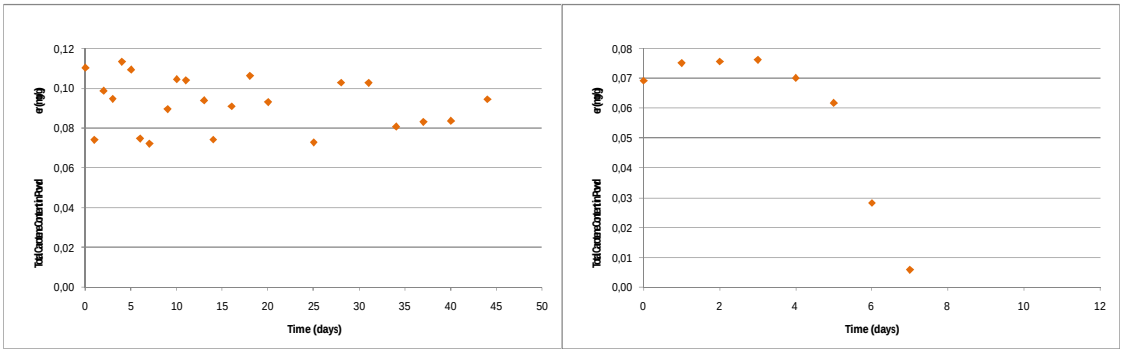


Figure A.4: Variation of the total carotene content (left) and surface carotene (right) of the encapsulate hydrated under an $a_w$ of 0,592.

## B. FULL DYNAMIC MECHANICAL ANALYSIS (DMA) RESULTS

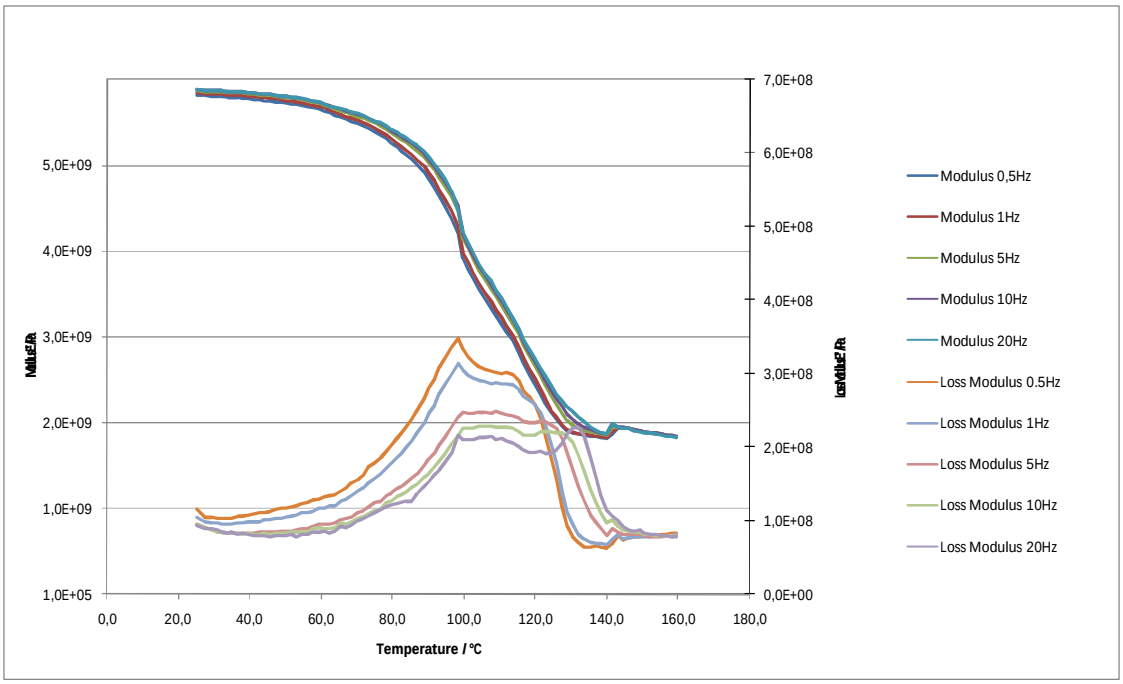


Figure B.1: Storage modulus (E') and loss modulus (E'') curves versus temperature, obtained by DMA on a amorphous lactose-trehalose sugar system, hydrated under a $a_w$ of 0,00 (First replicate).

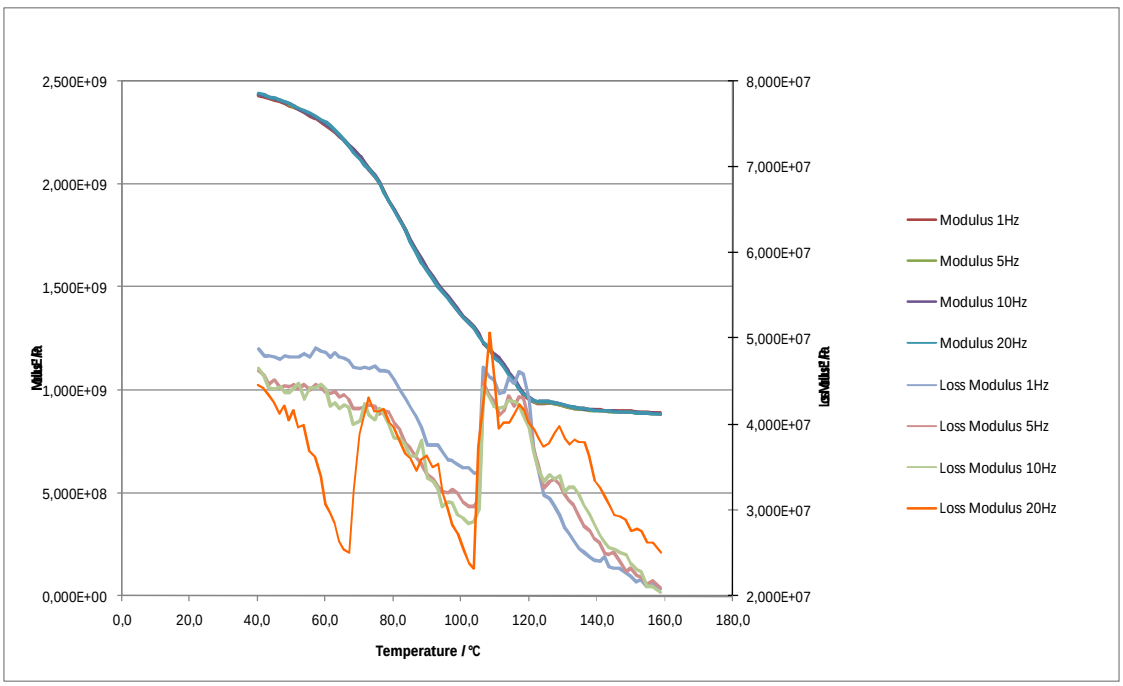


Figure B.2: Storage modulus (E') and loss modulus (E'') curves versus temperature, obtained by DMA on a amorphous lactose-trehalose sugar system, hydrated under a $a_w$ of 0,00 (Second replicate).

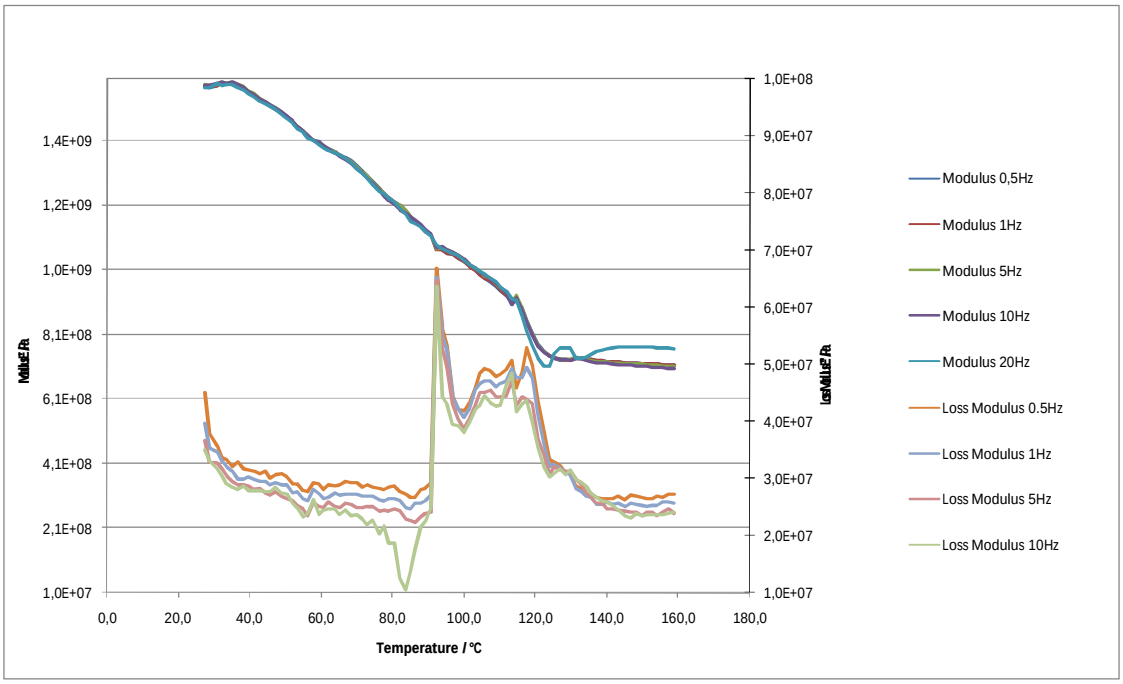


Figure B.3: Storage modulus (E') and loss modulus (E'') curves versus temperature, obtained by DMA on a amorphous lactose-trehalose sugar system, hydrated under a $a_w$ of 0,00 (Third replicate).

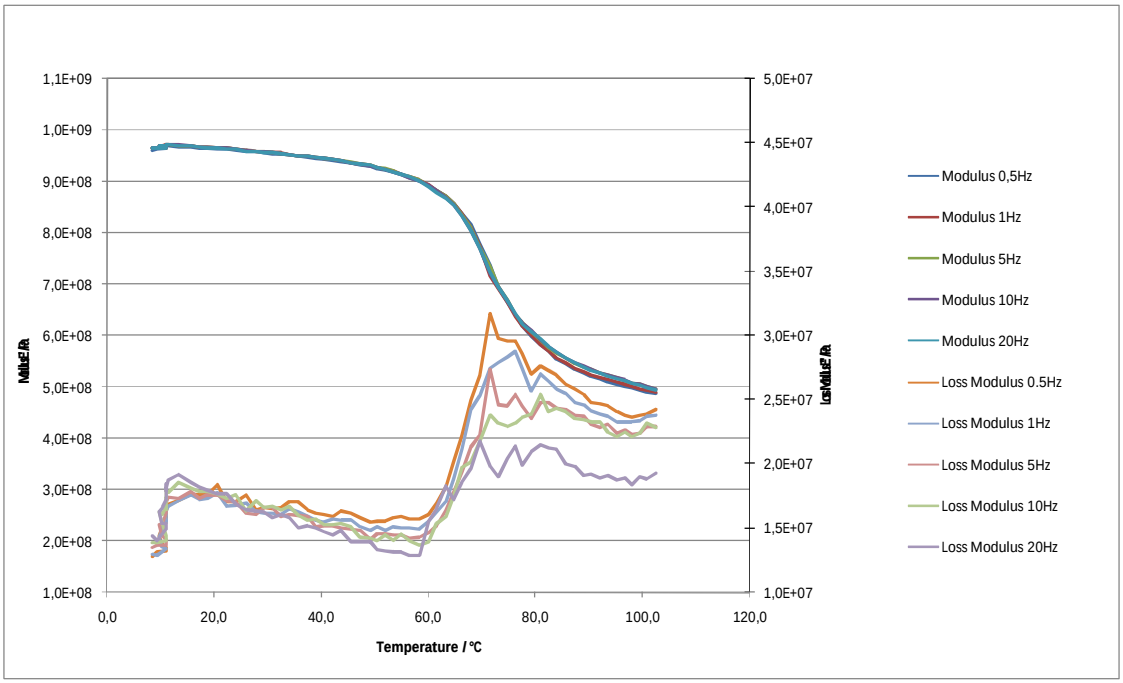


Figure B.4: Storage modulus (E') and loss modulus (E'') curves versus temperature, obtained by DMA on a amorphous lactose-trehalose sugar system, hydrated under a $a_w$ of 0,11 (First replicate).

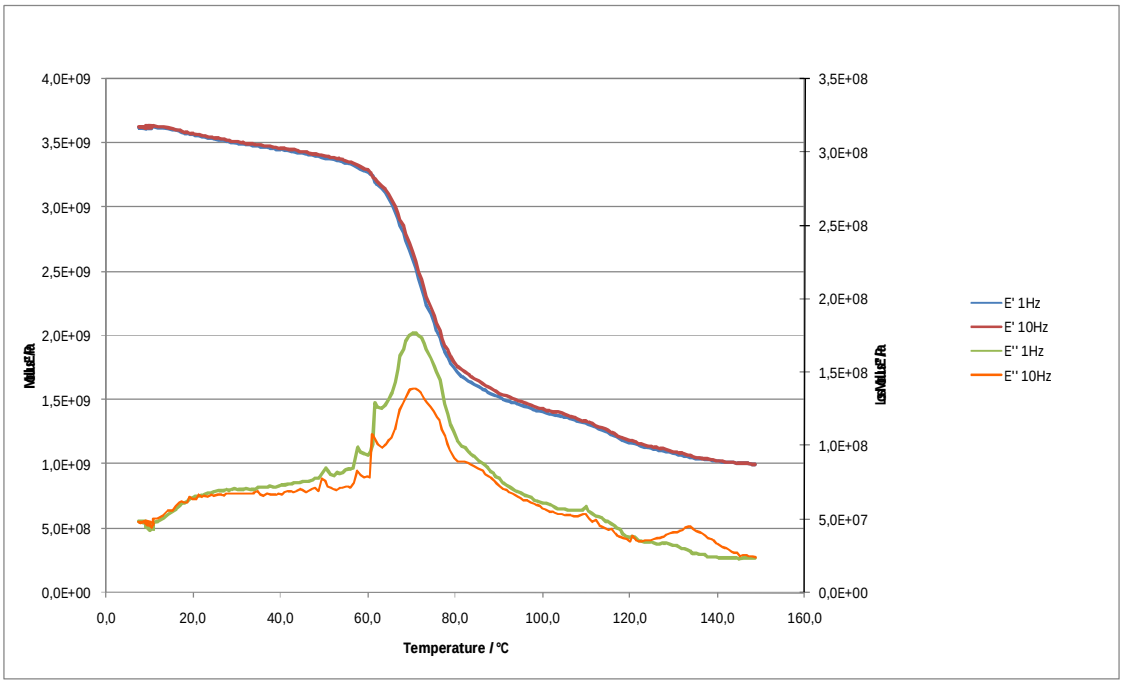


Figure B.5: Storage modulus (E') and loss modulus (E'') curves versus temperature, obtained by DMA on a amorphous lactose-trehalose sugar system, hydrated under a $a_w$ of 0,11 (Second replicate).

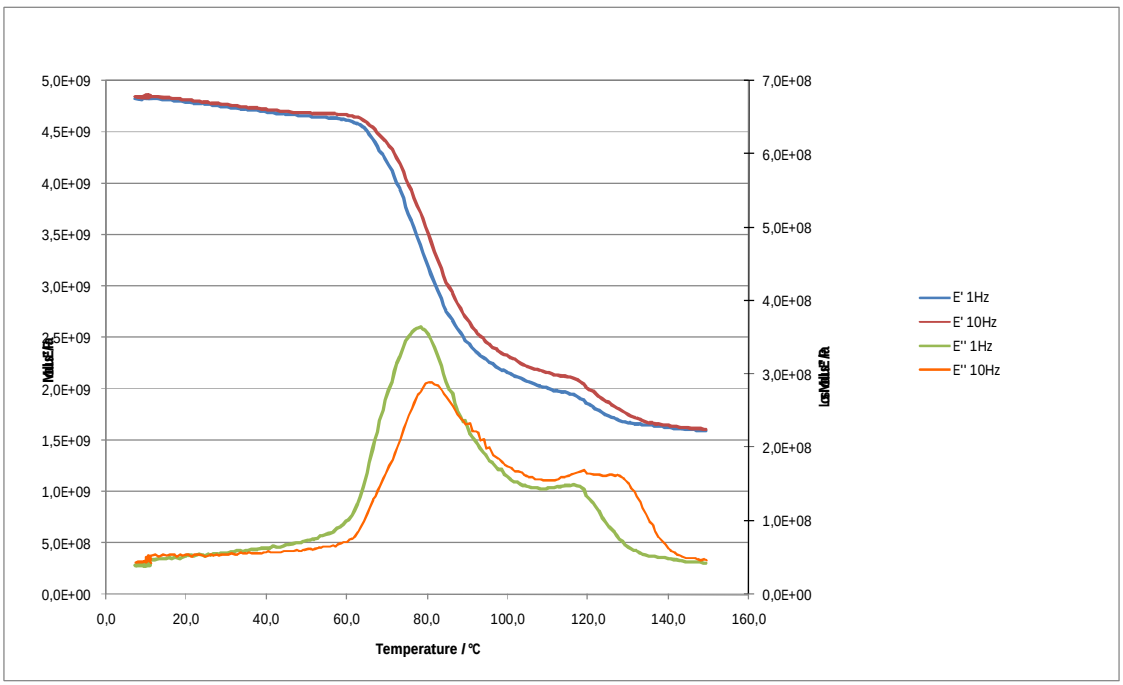


Figure B.6: Storage modulus (E') and loss modulus (E'') curves versus temperature, obtained by DMA on a amorphous lactose-trehalose sugar system, hydrated under a $a_w$ of 0,11 (Third replicate).

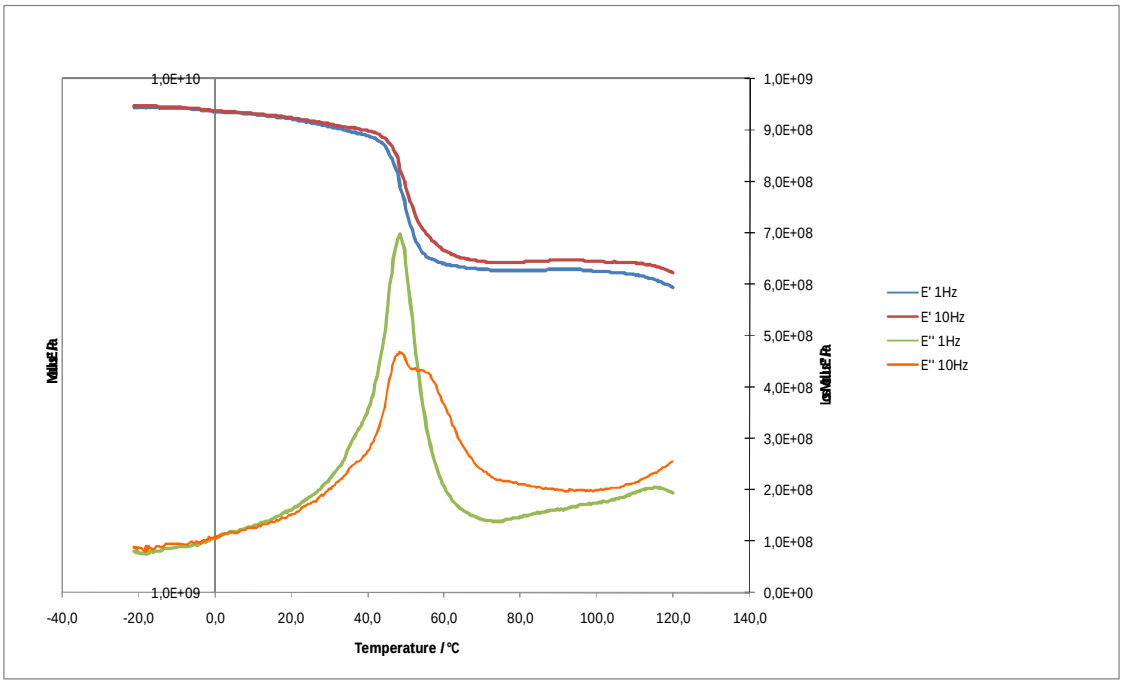


Figure B.7: Storage modulus (E') and loss modulus (E'') curves versus temperature, obtained by DMA on a amorphous lactose-trehalose sugar system, hydrated under a $a_w$ of 0,33 (First replicate).

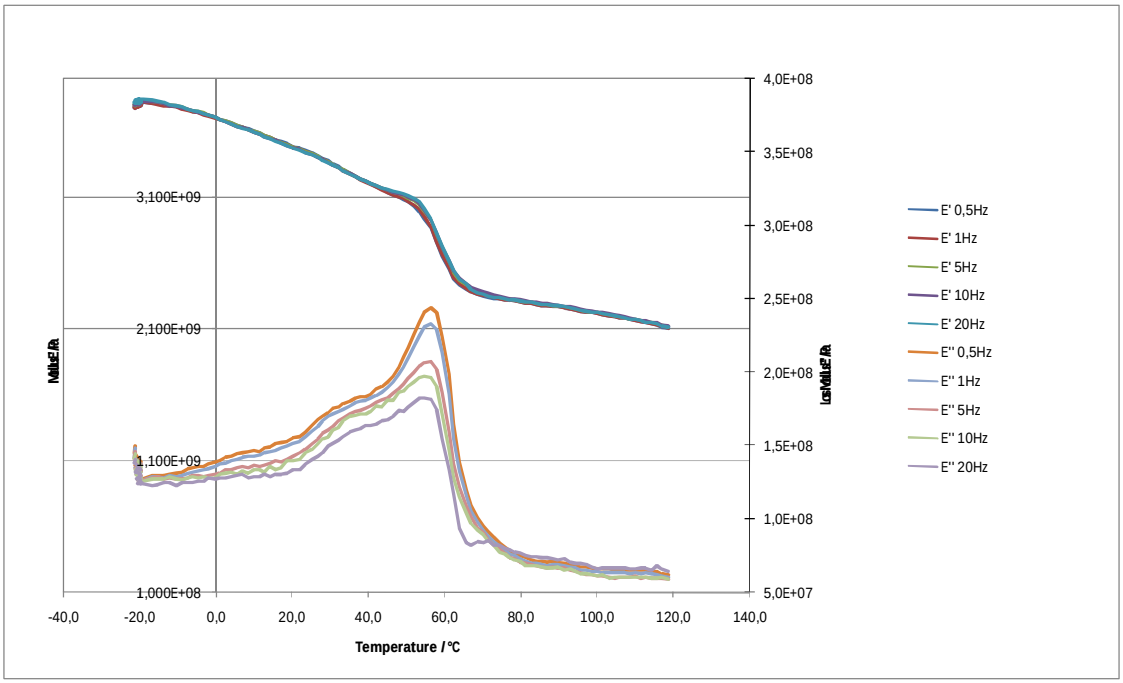


Figure B.8: Storage modulus (E') and loss modulus (E'') curves versus temperature, obtained by DMA on a amorphous lactose-trehalose sugar system, hydrated under a $a_w$ of 0,33 (Second replicate).

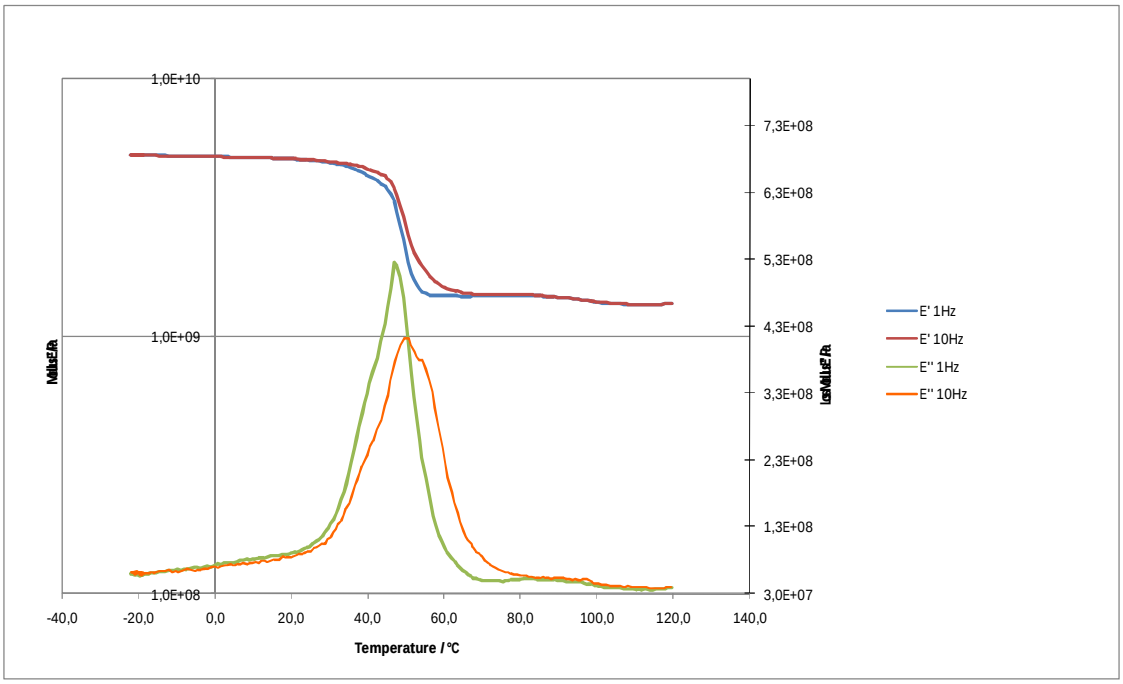


Figure B.9: Storage modulus (E') and loss modulus (E'') curves versus temperature, obtained by DMA on a amorphous lactose-trehalose sugar system, hydrated under a $a_w$ of 0,33 (Third replicate).

## C. FULL DI-ELECTRICAL ANALYSIS (DEA) RESULTS

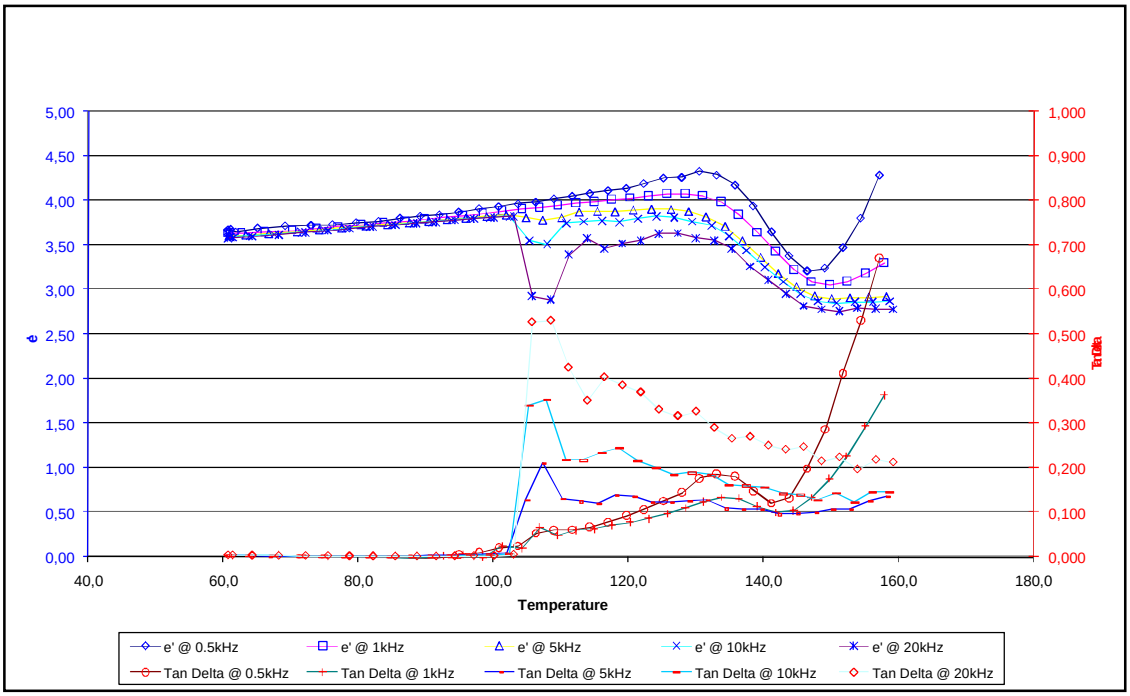


Figure C.1: Di-electric constant (ε') and loss tangent (tan δ) curves versus temperature, obtained by DEA on a amorphous lactose-trehalose sugar system, hydrated under a $a_w$ of 0,00 (First replicate).

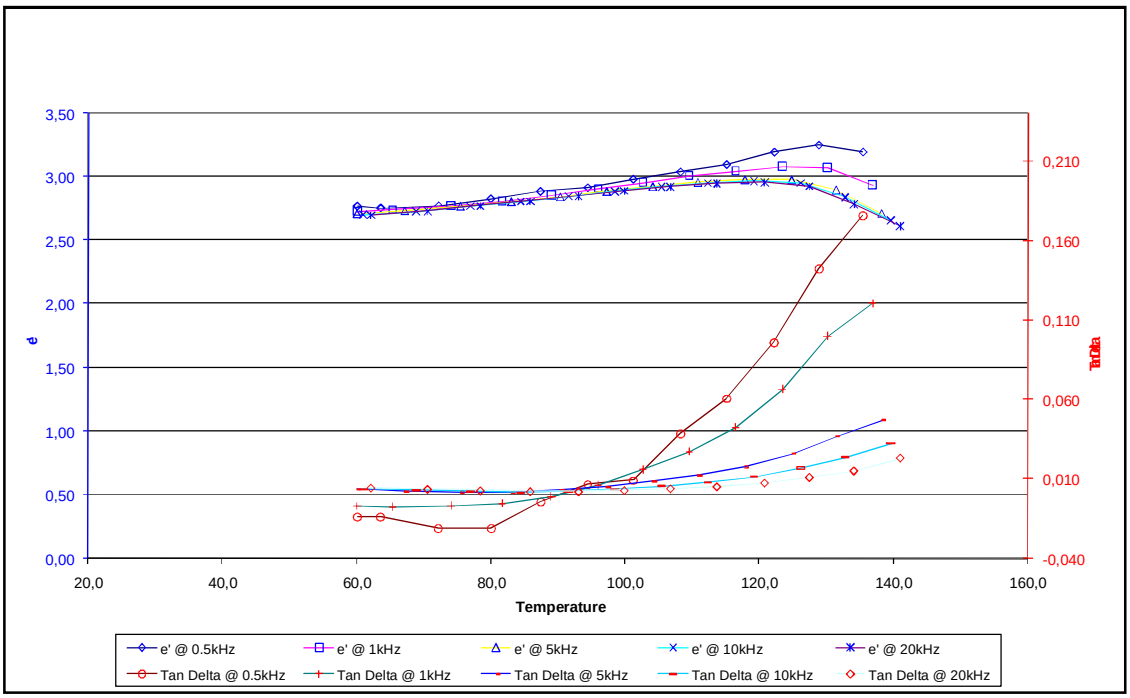


Figure C.2: Di-electric constant (ε') and loss tangent (tan δ) curves versus temperature, obtained by DEA on a amorphous lactose-trehalose sugar system, hydrated under a $a_w$ of 0,00 (Second replicate).

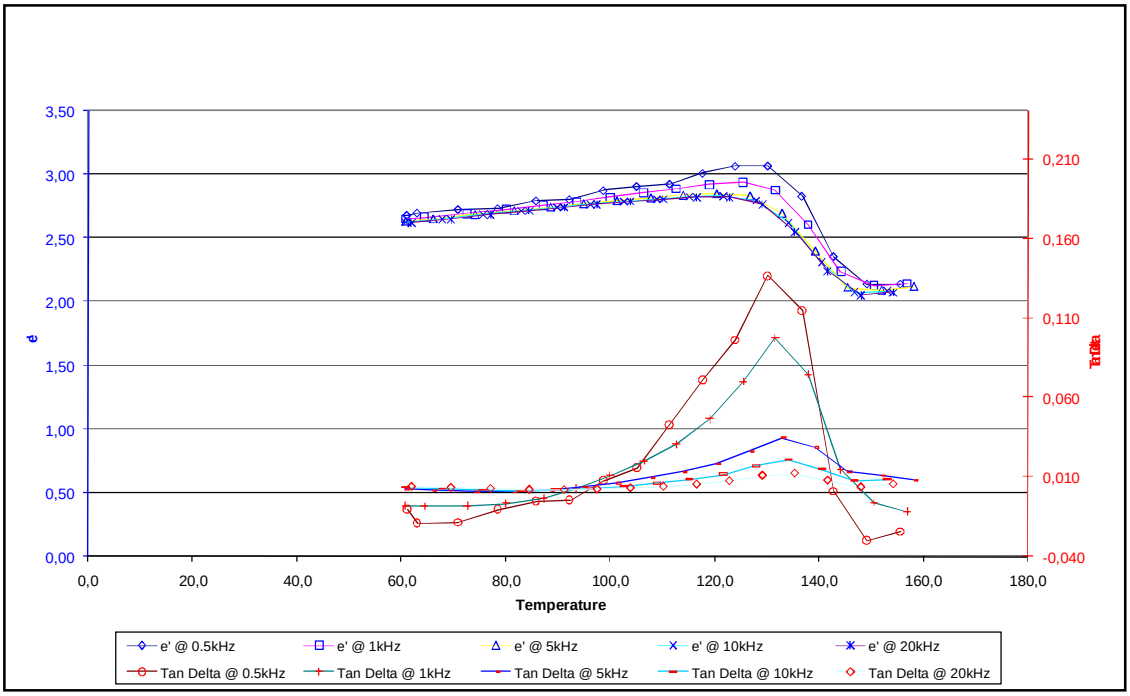


Figure C.3: Di-electric constant (ε') and loss tangent (tan δ) curves versus temperature, obtained by DEA on a amorphous lactose-trehalose sugar system, hydrated under a $a_w$ of 0,00 (Third replicate).

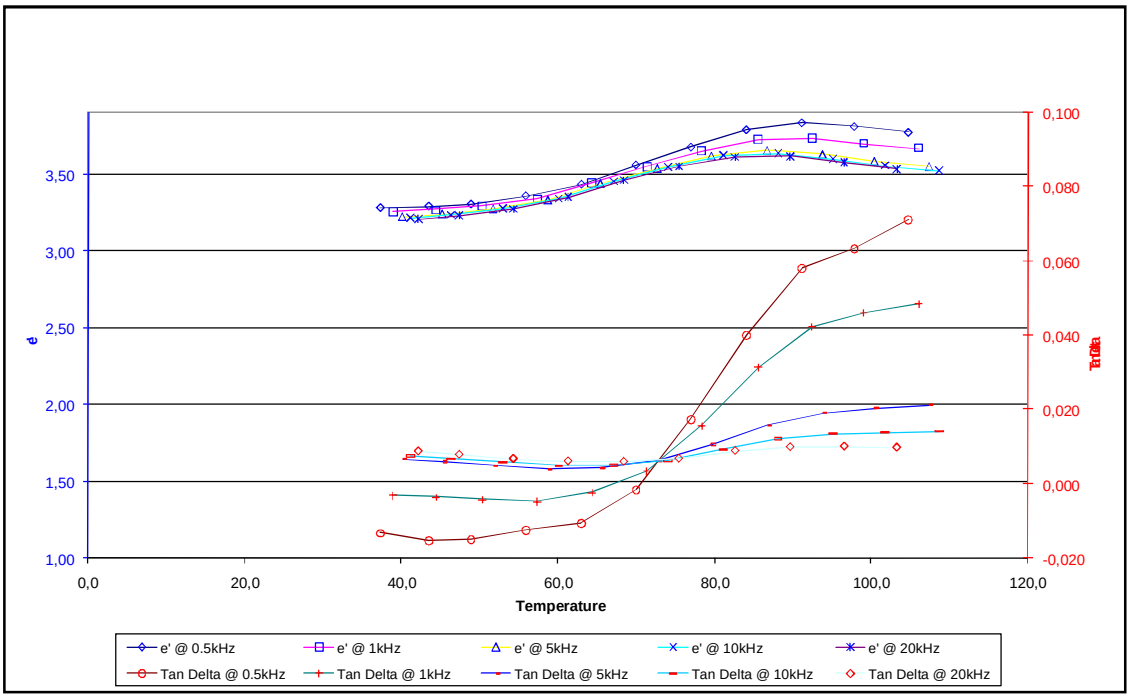


Figure C.4: Di-electric constant (ε') and loss tangent (tan δ) curves versus temperature, obtained by DEA on a amorphous lactose-trehalose sugar system, hydrated under a $a_w$ of 0,11 (First replicate).

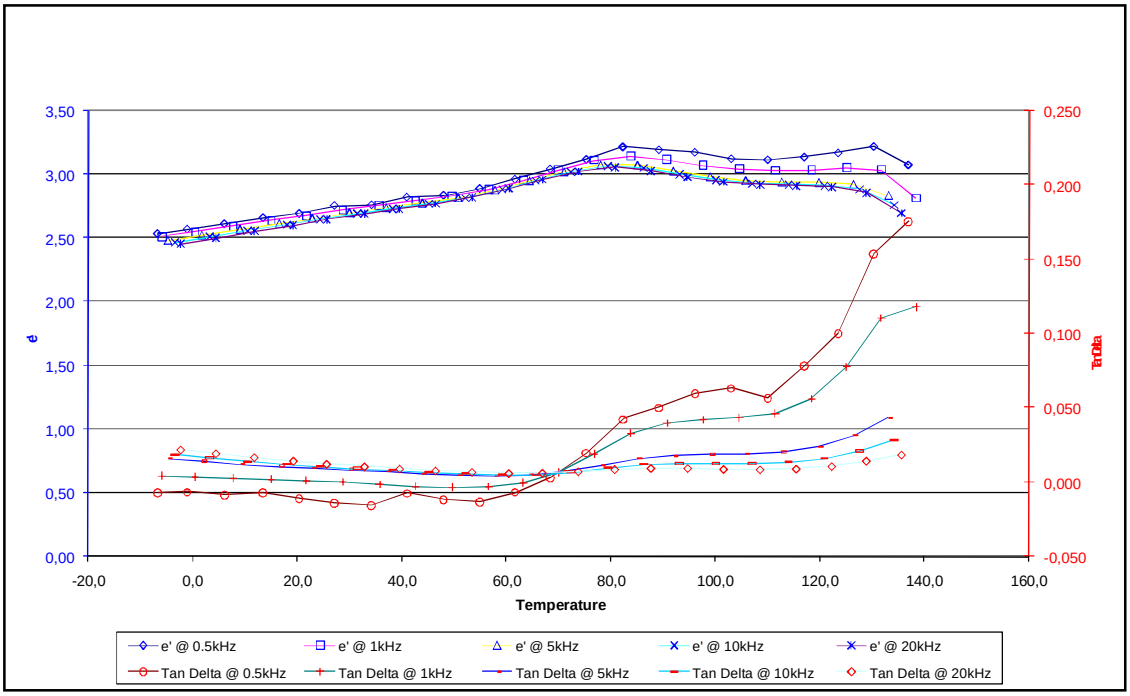


Figure C.5: Di-electric constant (ε') and loss tangent (tan δ) curves versus temperature, obtained by DEA on a amorphous lactose-trehalose sugar system, hydrated under a $a_w$ of 0,11 (Second replicate).

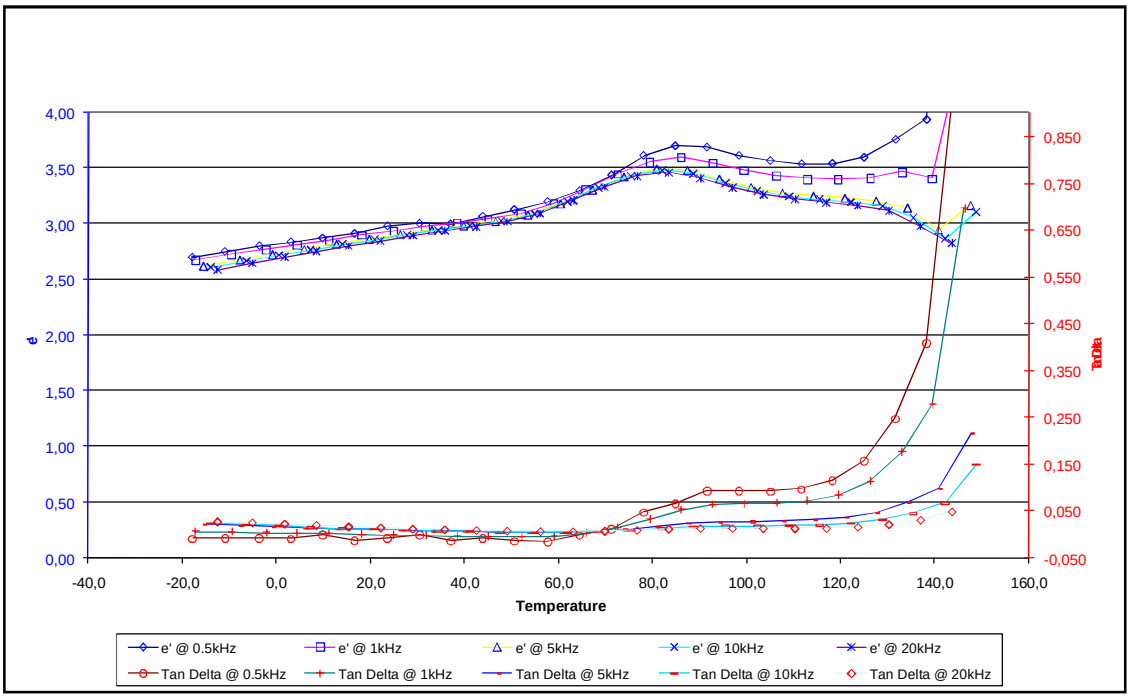


Figure C.6: Di-electric constant (ε') and loss tangent (tan δ) curves versus temperature, obtained by DEA on a amorphous lactose-trehalose sugar system, hydrated under a $a_w$ of 0,11 (Third replicate).

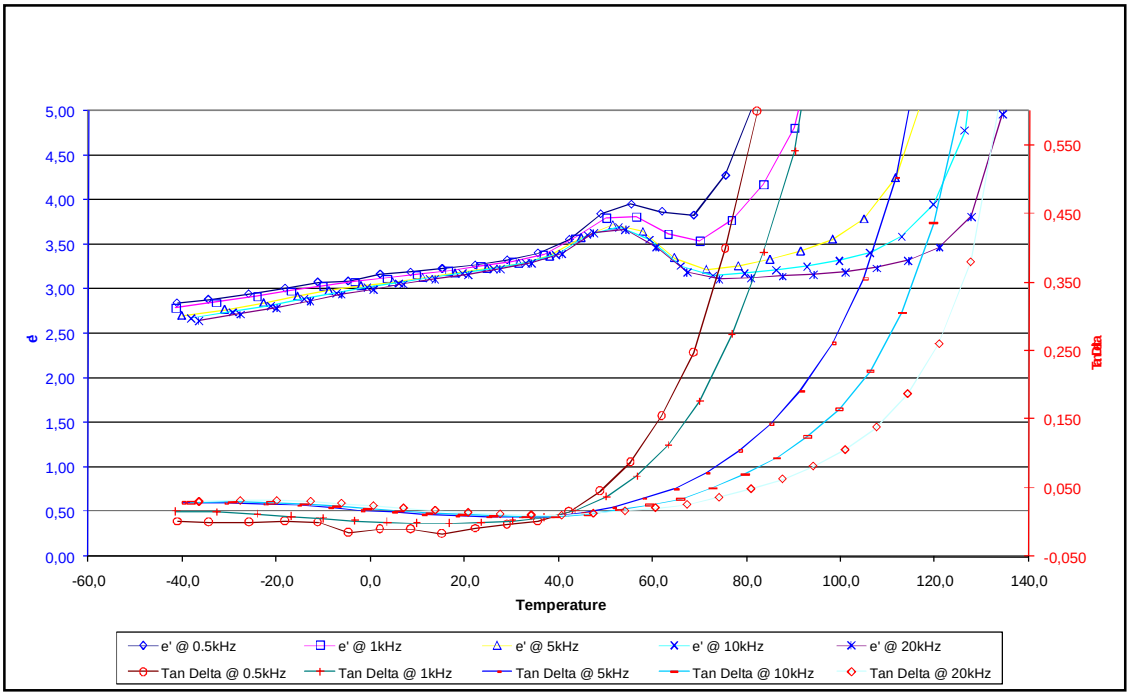


Figure C.7: Di-electric constant (ε') and loss tangent (tan δ) curves versus temperature, obtained by DEA on a amorphous lactose-trehalose sugar system, hydrated under a $a_w$ of 0,33 (First replicate).

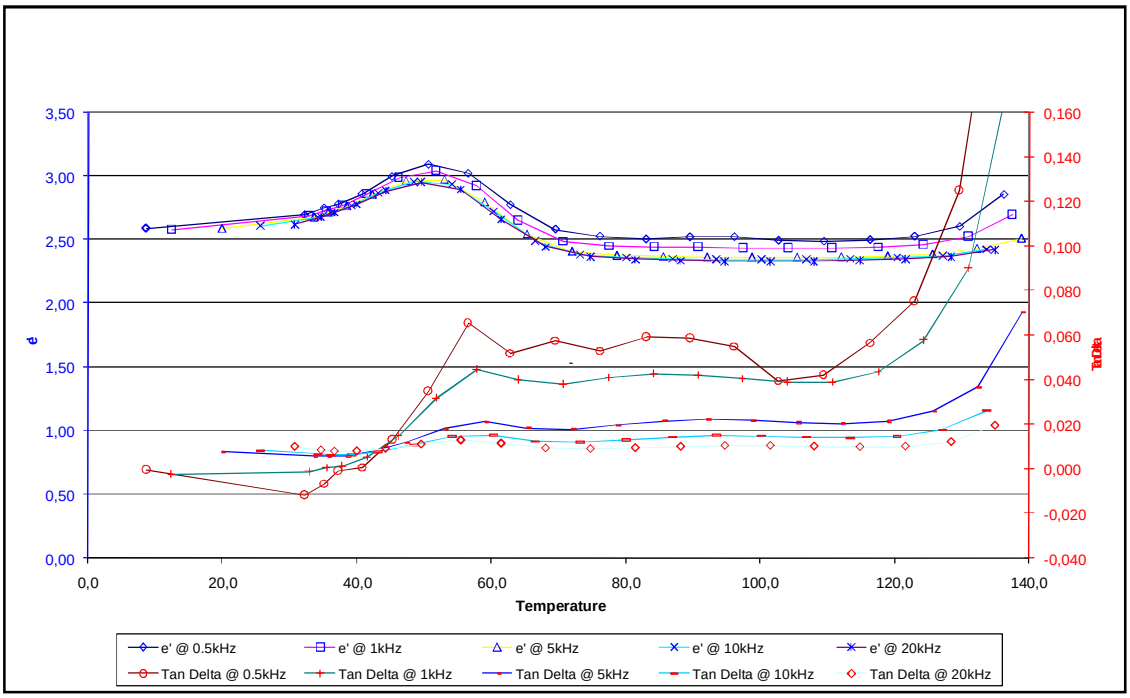


Figure C.8: Di-electric constant (ε') and loss tangent (tan δ) curves versus temperature, obtained by DEA on a amorphous lactose-trehalose sugar system, hydrated under a $a_w$ of 0,33 (Second replicate).

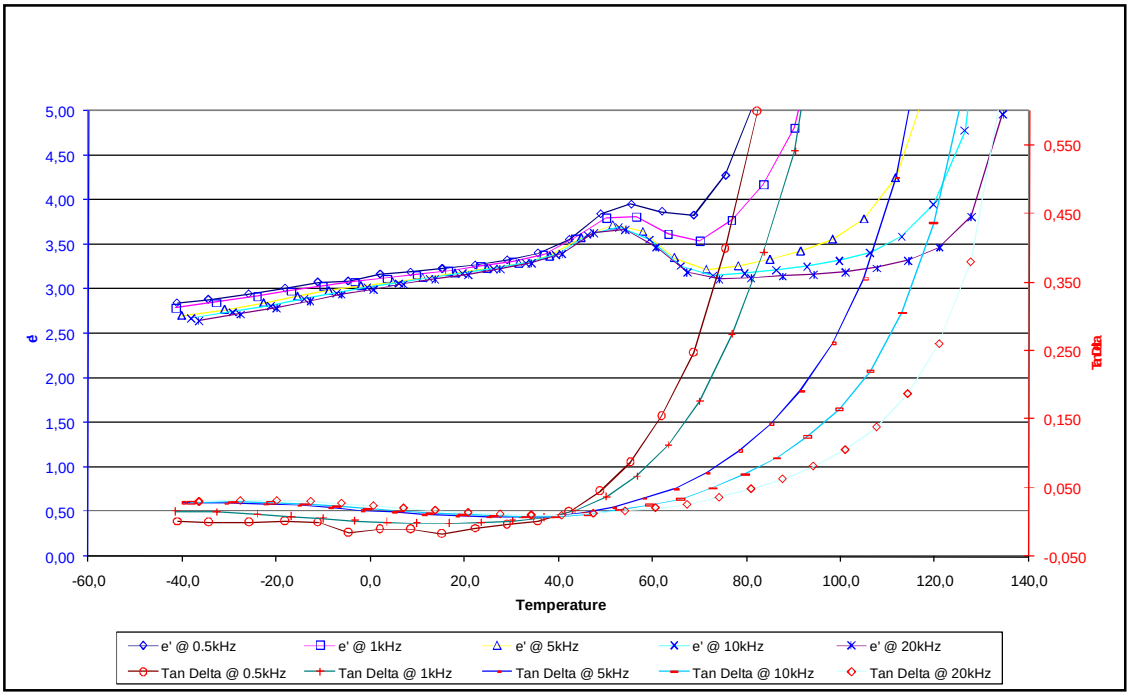


Figure C.9: Di-electric constant (ε') and loss tangent (tan δ) curves versus temperature, obtained by DEA on a amorphous lactose-trehalose sugar system, hydrated under a $a_w$ of 0,33 (Third replicate).

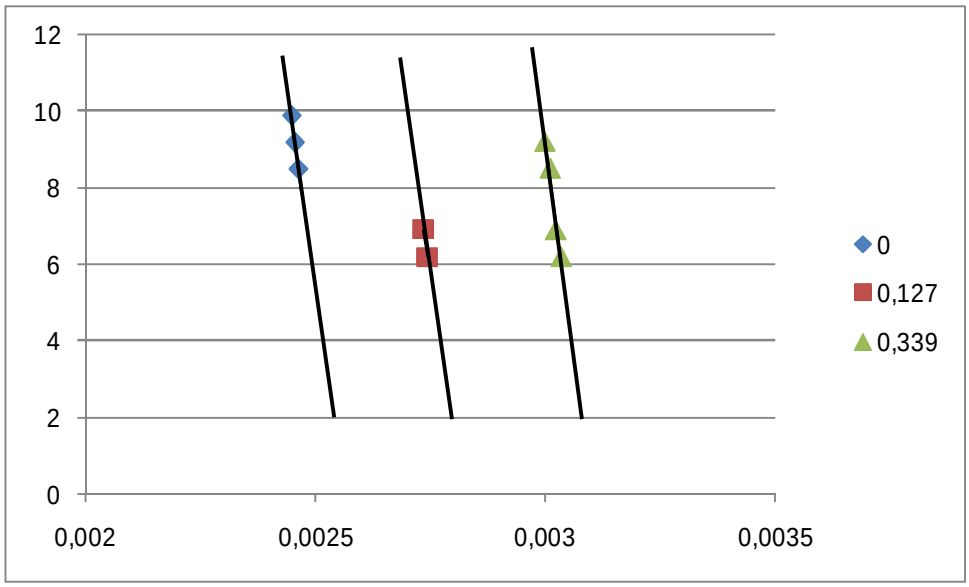


Figure C.10: Arrhenius plots of the DEA results, showing the linear relation between frequency of deformation and tan δ peak.